Analysis of Reduced and Oxidized Nitrogen-Containing Organic Compounds at a Coastal Site in Summer and Winter

Jenna C. Ditto[1,†], Jo Machesky[1], and Drew R. Gentner[1,*]

[1] Department of Chemical and Environmental Engineering, Yale University, New Haven, CT, 06511, USA

[†] Now at: Department of Chemical Engineering and Applied Chemistry, University of Toronto, Toronto, ON, M5S 3E5, Canada

* Correspondence to: drew.gentner@yale.edu

Abstract

Nitrogen-containing organic compounds, which may be directly emitted to the atmosphere or may form via reactions with prevalent reactive nitrogen species (e.g., NH_3, NO_x, NO_3), have important but uncertain effects on climate and human health. Using gas and liquid chromatography with soft ionization and high-resolution mass spectrometry, we performed a molecular-level speciation of functionalized organic compounds at a coastal site on the Long Island Sound in summer (during the LISTOS 2018 campaign) and winter. This region often experiences poor air quality due to the emissions of reactive anthropogenic, biogenic, and marine-derived compounds and their chemical transformation products. We observed a range of functionalized compounds containing oxygen, nitrogen, and/or sulfur atoms resulting from these direct emissions and chemical transformations, including photochemical and aqueous-phase processing that were more pronounced in summer and winter, respectively. In both summer and winter, nitrogen-containing organic aerosols dominated the observed distribution of functionalized particle-phase species ionized by our analytical techniques, with 85% and 68% of

total measured ion abundance containing a nitrogen atom, respectively. Nitrogen-containing particles included reduced nitrogen functional groups (e.g., amines, imines, azoles) and common NO_z contributors (e.g., organonitrates). The prevalence of reduced nitrogen functional groups observed in the particle-phase, while frequently paired with oxygen-containing groups elsewhere on the molecule, often rivaled that of oxidized nitrogen groups detected by our methods. Supplemental gas-phase measurements, collected on adsorptive samplers and analyzed with a novel liquid chromatography-based method, suggest that gas-phase reduced nitrogen compounds are possible contributing precursors to the observed nitrogen-containing particles. Altogether, this work highlights the prevalence of reduced nitrogen-containing compounds in the less-studied Northeastern U.S., and potentially in other regions with similar anthropogenic, biogenic, and marine source signatures.

1. Introduction

Coastal regions near the Long Island Sound often experience poor air quality due to a combination of biogenic and anthropogenic emissions from upwind metropolitan areas along the East Coast of the U.S. It is well established that these emissions undergo chemical transformations to form secondary pollutants during hours to days of over-water transport to downwind locations, including the states of Connecticut, Rhode Island, and Massachusetts (e.g., Cleveland et al., 1976). Emissions of gas-phase organic compounds (e.g., volatile, intermediate, and semi-volatile organic compounds (VOCs, IVOCs, SVOCs)) and primary organic aerosols (POA) are oxidized via numerous pathways in the atmosphere to yield ozone (O_3) and secondary organic aerosol (SOA) (Hallquist et al., 2009). SOA constitutes a variable but significant fraction of particulate matter with a diameter of 2.5 μm or less (i.e., $PM_{2.5}$). Both O_3 and $PM_{2.5}$ are of

47 particular concern for human health and climate; O_3 is known to cause an increase in respiratory-
48 related illnesses (Di et al., 2017; Jerrett et al., 2009), while $PM_{2.5}$ is known to cause adverse
49 cardiovascular, respiratory, and cognitive effects and to impact climate forcings (Di et al., 2017;
50 Hallquist et al., 2009; Kilian and Kitazawa, 2018; Pope and Dockery, 2006). Coupled with local
51 emissions and chemistry, these incoming aged air parcels from coastal metropolitan areas
52 contribute to the Long Island Sound region often entering nonattainment for O_3 (United States
53 Environmental Protection Agency, 2020), especially in the summer.

54 The chemistry and composition of organic compound emissions and secondary
55 transformation products in the Long Island Sound area is historically understudied, though some
56 past work has advanced our understanding of important sources and chemical pathways in the
57 region. For example, VOC and sub-micron particulate matter composition were investigated
58 during the 2002 New England Air Quality Study (de Gouw et al., 2005), with further VOC
59 speciation in 2004 during the New England Air Quality Study – Intercontinental Transport and
60 Chemical Transformation campaign (Warneke et al., 2007). More recently, a 2015 aircraft
61 campaign in the Northeast U.S. called WINTER characterized wintertime chemistry in the region
62 and also investigated organic aerosol formation via aerosol mass spectrometry (Schroder et al.,
63 2018). Finally, the LISTOS campaign in 2018 focused on measuring and modeling O_3 mixing
64 ratios over the Sound to investigate the dynamics of O_3 formation linked to large metropolitan
65 areas along the coast and associated downwind impacts (Zhang et al., 2020).

66 However, little is known about the molecular-level chemical composition of the gas-
67 phase I/SVOCs and functionalized organic aerosol formed in the Northeastern U.S. This
68 molecular-level speciation is key to understanding the physical/chemical properties of these
69 compounds in the atmosphere and their chemical transformations, especially for classes of

compounds containing reduced and oxidized nitrogen functional groups, whose emissions, lifetime, and ultimate impacts are generally poorly understood. For example, nitrogen-containing compounds that serve as reservoir species for nitrogen oxides may increase the overall lifetime of nitrogen oxides in the atmosphere via renoxification mechanisms (e.g., the photolysis of particulate nitrates, which has been studied in the marine boundary layer (Ye et al., 2016)); some may act as light absorbing chromophores (e.g.. the brown carbon studied from a methylglyoxal and ammonium sulfate system, which yielded mostly N-containing chromophores (Lin et al., 2015)); and some may have adverse, but uncertain, effects on human health (e.g., impacts on immune response to allergens (Ng et al., 2017)).

There have been a wide range of measurements of organic nitrogen in the atmosphere, and many past studies have emphasized enhancements in the contribution of this organic nitrogen in various forms of water in the atmosphere such as cloud water, fog water, rain water, and aerosol liquid water. For example, in cloud water, observations of important contributions from nitrogen- and oxygen-containing organic compounds have been made using Fourier-transform ion cyclotron resonance mass spectrometry (FT ICR-MS) (Zhao et al., 2013). Across all the oxygenates (i.e., CHO), oxygen- and nitrogen-containing compounds (CHON), oxygen- and sulfur-containing compounds (CHOS), and oxygen-, nitrogen-, and sulfur-containing compounds (CHONS) that Zhao et al. (2013) observed in cloud water, roughly 65% of ions (by number count) contained a nitrogen atom. Roughly half of all species observed were CHON compounds. Also, roughly half of the CHON species had low O/C (<0.7), and were hypothesized to contain reduced nitrogen functional groups. Another example from a study in the Southeastern U.S. by Boone et al. (2015) showed that cloud water samples contained a large fraction of nitrogenated species relative to aerosol-phase samples. From a combination of direct infusion

93 electrospray ionization and nanospray desorption electrospray ionization measurements with
94 high resolution mass spectrometry, Boone et al. (2015) observed roughly four times more CHON
95 molecular formulas in cloud water than in particle-phase samples, representing ~20% of all ions,
96 by number count, in cloud water. They also suggested an important role for aqueous-phase
97 reactions occurring between water-soluble oxygenated organic compounds and a diversity of
98 nitrogen-containing species such as ammonium, nitrate, small amines, among others (Boone et
99 al., 2015).
100 Similar observations have been made in fog water samples. For example, LeClair et al.
101 (2012) discussed the importance of water-soluble organic nitrogen-containing compounds in fog
102 water using FT ICR-MS. Roughly half of their observed compounds contained a nitrogen atom,
103 and by tracking neutral losses, they identified that 50-83% of their observed CHON species
104 showed a neutral loss of HNO_3 and thus likely contained a nitrate group. They noted that in the
105 absence of HNO_3, CH_3NO_3, NO, or NO_2 losses, the remaining nitrogen-containing ions observed
106 likely contained reduced nitrogen groups such as amine, amino, or imine structures (LeClair et
107 al., 2012). Another study of fog droplets with aerosol mass spectrometry by Kim et al. (2019)
108 showed an enrichment of organic nitrogen in fog droplets, including observations of reduced
109 nitrogen groups such as imidazoles and pyrazines (Kim et al., 2019). They observed fog water's
110 N/C ratio to be roughly 4 times greater than the N/C ratio in oxygenated organic aerosol samples.
111 These trends extend to rain water as well; FT ICR-MS measurements of rainwater in the
112 Northeastern U.S. by Altieri et al. (2009) showed large contributions of nitrogen-containing
113 organic compounds (Altieri et al., 2009). Approximately 70% of their observed nitrogen-
114 containing species were CHON species from positive mode ionization, which they suggested
115 consisted largely of reduced nitrogen functional groups based on their detection in positive

ionization mode and based on their elemental ratios. Similar enhancements in bulk organic nitrogen, made by measuring total nitrogen content and subtracting the contribution from inorganic nitrogen, were noted in both rain water and aerosols collected on the Mediterranean coast (Mace et al., 2003a), and in both rain and cloud water in a Caribbean background marine environment (Gioda et al., 2011).

While Boone et al. (2015) showed enhanced nitrogen content in cloud water relative to aerosol particles, aerosol-phase samples have also been observed in other studies across the globe to contain high organic nitrogen content. For example, at another location in the Southeastern U.S. with strong marine and continental air influence, Lin et al. (2010) observed that organic nitrogen in $PM_{2.5}$ contributed roughly 33% of total $PM_{2.5}$ nitrogen mass, which they computed by subtracting inorganic nitrogen contributions from total nitrogen content, as mentioned above (Lin et al., 2010). Similarly, 61% of primary marine aerosols (magnitude-weighted) collected from a ship in the Atlantic ocean and analyzed by FT ICR-MS were shown to contain nitrogen, and 54% of these primary marine aerosol species were CHON compounds, with the remaining 7% of nitrogen content distributed across CHONS and CHONP species (Wozniak et al., 2014). These primary marine aerosols typically had O/C ratios less than 0.5 and were also likely reduced nitrogen-containing, consistent with Zhao et al. (2013). Other examples include bulk organic nitrogen measurements from aerosols collected inland during both the wet and dry seasons in the Amazon basin (Mace et al., 2003b), from aerosols sampled in Davis, California (Zhang et al., 2002), and from aerosols (and fog) in the Po Valley in Italy (Montero-Martínez et al., 2014).

Finally, a recent study of aerosols collected in a forest in Tokyo highlighted the role of aerosol liquid water as another important medium for the formation of water soluble organic

nitrogen-containing species, and showed a positive correlation between the concentration of aerosol liquid water and water-soluble organic nitrogen (Xu et al., 2020).

Considering the coastal nature of our Long Island Sound site and general prevalence of water in the local/regional atmosphere (e.g., as cloud water, fog water, rain water, and aerosol liquid water), the overall goal of this study was to examine the composition and contributions of nitrogen-containing organic compounds from mixed anthropogenic, biogenic, and marine sources, as well as the possible roles of secondary product formation via aqueous-phase chemistry. We collected samples of organic gases and particles for detailed chemical speciation on the coast of the Long Island Sound in Guilford, Connecticut. We note that we used this site as a case study, but our observations of emissions and chemistry at this site are likely informative for other coastal urban and downwind regions due to the ubiquity of nitrogen-containing emissions from anthropogenic, biogenic, and marine sources.

Samples were collected during the summer and winter, and analyzed via high resolution mass spectrometry to speciate the complex mixture of emissions and chemical transformation products. These samples were taken alongside several targeted pollutant measurements including O_3, nitrogen oxides (NO_x), particulate matter with a diameter of ≤ 2.5 μm ($PM_{2.5}$), and black carbon (BC), all to inform our chemically-speciated analyses, and to contribute to a longer-term characterization of this coastal area.

The specific objectives of this study were to: (1) investigate compositional differences and possible chemical pathways contributing to measured summer and winter functionalized organic aerosols at this site; (2) examine the relative contributions of reduced and oxidized nitrogen groups to functionalized organic aerosol; and (3) use a novel sampling and liquid chromatography-based analytical approach to probe the molecular-level composition of

functionalized gas-phase organic compounds and investigate possible nitrogen-containing gas-phase precursors to the observed reduced nitrogen-containing particles.

2. Materials and Methods

We collected measurements at the Yale Coastal Field Station (YCFS) in Guilford, Connecticut (41.26°N, 72.73°W) (Rogers et al., 2020). Inlets were positioned facing the Long Island Sound (i.e., South-Southeast) to capture onshore flow. The YCFS often received aged urban incoming air from East Coast metropolitan areas, similar to known common air parcel trajectories in the region (Figure S1). However, due to extensive mixing in the Northeast corridor and over the Long Island Sound, along with extended collection times for offline gas- and particle-phase samples, we also observed considerable biogenic and anthropogenic influence from other areas of the Northeastern U.S.

2.1. Offline Samples of Organic Particles and Gases Analyzed via Liquid and Gas Chromatography with Mass Spectrometry

We discuss three types of sampling and quadrupole time-of-flight mass spectrometry-based analyses here: particles collected on Teflon filters and analyzed using liquid chromatography with electrospray ionization, gases collected on packed adsorbent tubes and analyzed using gas chromatography with atmospheric pressure chemical ionization, and functionalized gases collected on cooled polyether ether ketone (PEEK) samplers and analyzed using liquid chromatography with electrospray ionization. Teflon filter and adsorbent tube measurements were collected at the YCFS during the summer as part of the 2018 Long Island Sound Tropospheric Ozone Study (LISTOS), from July 9 to August 29, 2018. Additional filter

and adsorbent tube samples were collected during the following winter from February 25 to March 5, 2019. Supplemental wintertime gas-phase samples on PEEK tubing were collected briefly from March 5-6 2020, prior to the COVID-19 shutdown. These sampling periods are discussed here as summer and winter case studies but longer campaigns are warranted to assess full seasonal trends.

A custom filter and adsorbent tube housing was constructed to simultaneously collect particle- and gas-phase organic compounds, respectively (Sheu et al., 2018). The filter was positioned immediately upstream of the adsorbent tube to collect particles for analysis and to prevent particles from reaching the gas-phase adsorbent tube sample. The housing was designed to minimize spacing between the filter and adsorbent tube to reduce gas-phase losses to upstream surfaces, and was built out of a modified passivated stainless steel filter holder (Pall) and an aluminum block with sealed 6.34 mm (1/4") holes for adsorbent tubes (Sheu et al., 2018).

For filter and adsorbent tube collection, we used a short inlet (0.9 m long, 5/8" OD stainless steel tubing, positioned 2.5 m above the ground) upstream of the custom sampler to allow the sampling media to be housed in an air-conditioned trailer. A stainless steel mesh screen (84 mesh) was used at the opening of the inlet to limit particle size to ~PM_{10} and to prevent large particles from entering the sampler (Ditto et al., 2018). Penetration efficiency through the mesh screen was computed for the 20 L/min flow rate using the screen thickness, mesh size (84 mesh), wire diameter, and accounting for the effects of diffusion, impaction, and interception. Based on this modeling, we expect roughly 50% penetration efficiency at PM_{10} and 0% at PM_{11} and larger.

2.1.1. Filter sampling, analysis, and data QA/QC

Teflon filters (47 mm, 2.0 μm pores, Tisch Scientific) were used for particle-phase sampling. Filters were collected at 20 L/min for 8 hours, during the day (9:00am-5:00pm) and at night (9:00pm-5:00am). Samples were extracted in methanol and analyzed via liquid chromatography (LC) using an Agilent 1260 Infinity LC and an Agilent Poroshell 120 SB-Aq reverse phase column (2.1 x 50 mm, 2.7 μm particle size). The LC was coupled to an electrospray ionization (ESI) source and a high-resolution mass spectrometer (Agilent 6550 Q-TOF), and operated following previously described methods (Ditto et al., 2018, 2020). The mass resolution (M/ΔM) of the Q-TOF used in this work was ≥25,000-40,000, and the mass accuracy was 1-2 ppm. Our use of LC (or GC) to separate compounds prior to their ionization and detection by the mass spectrometer reduced mass spectral interferences and thus enabled accurate molecular formula assignments beyond what would be possible by relying on the Q-TOF's mass resolution alone.

Filter extracts were run with MS (i.e., TOF-only, to identify molecular formulas) and MS/MS (i.e., tandem mass spectrometry, to identify functional groups) data acquisition, using both positive and negative mode electrospray ionization. These methods are hereafter referred to as "LC-ESI-MS" and "LC-ESI-MS/MS", respectively. Acquisition and non-targeted analysis methods, including data quality assurance and quality control (QA/QC), are discussed in past work (Ditto et al., 2018, 2020). Briefly, for LC-ESI-MS analyses, any ion mass appearing in both a sample and its corresponding blank (matching ion mass with a tolerance of 5 ppm, and matching ion retention time with a tolerance of 0.25 min—both tolerances were chosen to be quite conservative) was removed if its abundance in the sample was less than 5 times its abundance in the blank. Ions with greater sample:blank ratios were retained, and the abundance

of the blank peaks were subtracted from the sample peaks. Positive and negative ionization mode data were combined and any ions appearing in both modes were flagged; abundances were averaged and the compound was only counted once. Ions from m/z 50-600 were assigned formulas assuming hydrogen or sodium adducts in positive mode and acetate adducts or deprotonation in negative mode. We also allowed for the neutral loss of water. Only peaks that well-surpassed instrument noise and that had strong peak quality scores (based on both liquid chromatography and mass spectrometry data) were selected for formula identification according to thresholds detailed in Ditto et al. 2018. Formulas were assigned with the following elemental constraints in Agilent's Mass Hunter software: $C_{3-60}H_{4-122}O_{0-20}N_{0-3}S_{0-3,}$ minimizing the ppm mass difference between the observed and proposed ion mass and accounting for isotope distribution. Prior to non-targeted analysis, further QA/QC was performed on these formula identifications using custom R code. As discussed by Kind and Fiehn (2007), the number of elements was further constrained to 39 carbons and 72 hydrogens, and H/C ratios were checked to ensure they fell within expected limits ($0.2 < H/C < 3.1$) (Kind and Fiehn, 2007). Formulas were then screened to ensure they agreed with the Nitrogen rule, to ensure that all double bond equivalent values were integers, and to flag any large mass differences (>7 ppm) between the observed and proposed mass for a given molecular formula.

For MS/MS, any ions from the LC-ESI-MS analyses that passed these QA/QC steps were targeted for MS/MS fragmentation at 5, 10, 20, 30 and 40 V. We used SIRIUS with CSI:FingerID for functional group identification with a subset of compounds from MS analysis (Dührkop et al., 2015, 2019), as detailed in past work (Ditto et al., 2020). We assumed the same ionization behavior as discussed above, with the same elemental composition constraints and a conservative 7 ppm mass tolerance. Functional groups for the top-scoring candidate structure for

each ion were tallied with APRL Substructure Search Program (Ruggeri and Takahama, 2016). The exact position of each functional group was not considered, as the focus of our work was instead to assess the presence or absence of atmospherically relevant functional groups and their combinations across a large number of multifunctional compounds.

After stringent QA/QC for peak shape and accurate molecular formula determination, non-targeted compound identification from LC-ESI-MS identified an average of 200±56 and 167±47 compounds per sample analyzed in summer and winter, respectively, across 34 samples in summer and 15 in winter.

We note that filter ion abundance data is presented as combined positive and negative ionization mode data, which treats the compounds equally without corrections for ionization efficiency. As mentioned above, compounds were not double counted; any ion appearing in both positive and negative mode was flagged, its average abundance computed, and it was tallied only once. While ionization efficiency differences between compound types exist, their exact effects for multifunctional compounds present in a complex mixture are uncertain. Thus, similar to other studies and to our past work, we treat the intercomparison across compounds without adjusting for ionization efficiency differences (Ditto et al., 2018). We note that the figures in the main text are displayed as fractions of total observed ion abundance, to consider variations in atmospheric abundance across the complex mixture of functionalized species. However, due to uncertainty in exact ionization efficiency, these are not intended to directly represent mass concentration. For comparison, identical figures represented by occurrence (i.e., unweighted by abundance) are presented in the SI (Figures S4-S6, S8-S9, S11, S13); general observations remain similar between abundance weighted and occurrence results.

2.1.2. Adsorbent tube sampling, analysis, and data QA/QC

Gas-phase samples were collected on glass adsorbent tubes (6.35 mm OD, 88.9 mm long) packed with quartz wool, glass beads, Tenax TA, and Carbopack X (Sheu et al., 2018). Samples were collected at 200 mL/min for 2 hours, sub-sampling off of the 20 L/min filter flow, during the day (2:00-4:00pm) and at night (2:00-4:00am). Adsorbent tubes were analyzed using a GERSTEL TD3.5+ thermal desorption unit and an Agilent 7890B gas chromatograph (GC) with a DB5-MS UI column (30 m x 320 μm x 0.25 μm). The GC was coupled to an atmospheric pressure chemical ionization (APCI) source and the same Q-TOF as above, operated with MS (i.e., TOF-only) data acquisition and positive ionization mode only. These methods are hereafter called "GC-APCI-MS" and acquisition and analysis methods are discussed in past work (Ditto et al., 2021; Khare et al., 2019). After QA/QC (as detailed in Section 2.1.1), this non-targeted analysis yielded an average of 388±201 and 612±133 compounds per sample in summer and winter, respectively, across 34 samples in summer and 14 samples in winter.

2.1.1. PEEK collector sampling, analysis, and data QA/QC

Finally, as a supplemental analysis to probe the composition of functionalized gases that were not GC amenable and thus not measured using the adsorbent tube and thermal desorption-gas chromatography techniques mentioned above, we used PEEK-based sample collectors and liquid chromatography to trap and speciate oxygen-, nitrogen-, and/or sulfur-containing gases without thermal desorption. This method was designed to target functionalized gases, which represent important precursors, intermediates, and by-products in the atmospheric processing of emitted organic compounds but are often challenging to speciate with traditional GC techniques due to their chemical functionality, reactivity, and/or thermal lability. Additionally, in many gas-

phase measurement systems, primary emissions (i.e., hydrocarbons) can overwhelm the signal of more functionalized analytes, adding to the challenge of speciating these lower abundance compounds.

Thus, to probe the chemical composition of these functionalized gases, we used a sampling approach, desorption method, separation method, and ionization technique that leveraged their relatively lower volatility and higher polarity. This included adsorptive sampling onto cooled PEEK tubing followed by direct inline desorption into the LC mobile phase for LC-ESI-MS analysis. ESI was specifically chosen here because it is sensitive to functionalized compounds. Testing was performed in positive and negative ionization mode, but field samples were run in positive mode only. Further details and discussion of this method, including method development and evaluation, can be found in Section S1 and Tables S1-3. Briefly, PEEK tubing was cooled to 2°C and used as an adsorptive collector, with a Teflon filter positioned upstream of the PEEK tubing to remove particles. PEEK was selected due to its inert behavior, thus reducing the possibility for surface-analyte interactions that might inhibit effective inline solvent desorption and dissolution. PEEK is also compatible with the solvents used in the LC system, and is frequently used in LC instruments. Field samples were collected on cooled PEEK tubing during the subsequent winter (March 5-6, 2020), for 2 hours each between 8:00am-2:00pm. For these 2 hour (~2.6 L) field samples, functionalized gases in a typical 100-250 g/mol molecular weight range were resolvable at ~25-60 ppt in the atmosphere, based on instrument detection limits (Ditto et al., 2018). For analysis, each PEEK collector was installed in the LC system flow path, and analytes were directly desorbed using the LC mobile phase solvents then trapped and focused on the LC column for 20 minutes, before being analyzed using the same LC-ESI-MS system in positive ionization mode (Figure 1). This inline mobile phase desorption step gently

mobilized potentially fragile analytes from the PEEK collector and trapped and focused them on the LC column prior to chromatographic separation and mass spectral analysis. Additionally, this preconcentration step allows for the detection and characterization of lower concentration species. Data were processed and QA/QC were performed as detailed in Section 2.1.1.

We note that there are other existing approaches for offline collection of highly-functionalized organic gases and particles that are compatible with LC analysis such as spray chambers, particle into liquid samplers, coated denuders, PUF sampling, and more. This PEEK sampling method with inline desorption into the LC mobile phase was pursued to reduce sample preparation steps and thus possibilities for losses (e.g., during solvent extraction or evaporative preconcentration), as well as for its direct similarity to the filter-based particle-phase LC-ESI-MS analysis.

We also note that for all filter collection and LC analyses (filters and PEEK collectors), it is possible that some functional groups of interest may have undergone hydrolysis on the filter during 8-hour filter collection periods or in the LC mobile phase, which was primarily water at the beginning of the LC solvent gradient. For example, organonitrates may be susceptible to hydrolysis depending on their structure; tertiary organonitrates can undergo hydrolysis on the timescale of minutes-hours depending on pH, while primary/secondary organonitrates are relatively stable. Hydrolysis occurs more quickly at low pH. The pH of the LC mobile phase (pH ~ 2) and the pH of the sampled aerosol (pH < ~5, (Pye et al., 2020)) are both acidic; alpha-pinene-derived organonitrates, for example, could have a lifetime of as low as of roughly 8 minutes to 1.5 hours across this pH range (Rindelaub et al., 2016). If hydrolysis occurred, some of the observed compounds could be byproducts of other functionalized species. While we did

not observe any of our nitrogen-containing test standards to hydrolyze over these timescales, standards were not available to reflect every functional group observed in these datasets.

2.2. Supporting Measurements

O_3, NO_x, $PM_{2.5}$, and BC concentrations were recorded concurrently during both summer and winter sampling periods. O_3 was measured with a 2B Tech Model 202 Ozone Monitor, NO_x with a Thermo Scientific Model 42i-TL Analyzer, $PM_{2.5}$ with a MetOne BAM-1020 instrument, and BC with a Magee Scientific AE33 Aethalometer. O_3 and NO_x inlets were constructed of FEP tubing (1/4" OD), with a Teflon filter housed in a PFA filter holder upstream to remove particles. The $PM_{2.5}$ inlet was made of stainless steel tubing (1 ¼" OD) and the BC inlet was made of copper tubing (3/8" OD). Both particle inlets were outfitted with a $PM_{2.5}$ cyclone to limit particle size to 2.5 μm and below.

All inlets were mounted 3 m above the ground. Instrument flow rates were calibrated with an external mass flow controller. O_3 and NO_x monitors were zeroed with laboratory-generated zero air. The O_3 monitor was calibrated against Connecticut Department of Energy and Environmental Protection instrumentation and further confirmed with an O_3 generator in the lab. The NO_x monitor was calibrated using a NO standard (AirGas, 2 ppm NO in nitrogen, ± 5%) diluted to 25 ppb with laboratory-generated nitrogen gas. The BC instrument was programmed to conduct an automatic performance check using particle-free air and the $PM_{2.5}$ instrument was zeroed following MetOne protocols with particle-free air. O_3 and NO_x data were collected at 1-second intervals, BC data were collected at 1-minute intervals, and $PM_{2.5}$ data were collected at 1-hour intervals. BC data were saved directly from the instrument, while O_3, NO_x, and $PM_{2.5}$ data were recorded with a LabJack T7 datalogger and custom LabView code. In addition, hourly

368 weather data (temperature, relative humidity, wind speed, wind direction) were collected with a
369 WeatherHawk weather station on top of the 3 m tower.

370 During the summer, we also collected a small number of size-resolved particle samples
371 on quartz filters using an eight-stage cascade impactor (Thermo Scientific Andersen Non-Viable
372 Cascade Impactor). Sizes ranged from 0.43-10.0 μm (stage 0: 9.0-10.0 μm, stage 1: 5.8-9.0 μm,
373 stage 2: 4.7-5.8 μm, stage 3: 3.3-4.7 μm, stage 4: 2.1-3.3 μm, stage 5: 1.1-2.2 μm, stage 6: 0.65-
374 1.1 μm, stage 7: 0.43-0.65 μm). Quartz filters were extracted and analyzed following the same
375 procedure as the Teflon filters discussed above, with the addition of a syringe filtration step to
376 remove insoluble fibers. The cascade impactor was positioned on the roof of the trailer and
377 pulled 28.3 L/min (GAST 1531-107B-G557X pump) through the inlet for periods of 8 hours
378 during the day and at night (same timing as above).

379 Finally, we computed 48-hour backward trajectories for every hour during each offline
380 sample collection period with the HYSPLIT Backward Trajectory Model (accessed online at
381 https://www.ready.noaa.gov/HYSPLIT.php), using GDAS1.0 meteorological data, the field site's
382 coordinates as each trajectory's end point, and a final trajectory height of 50 m above the
383 ground. We selected 48 hours trajectories to focus on regional influence at the site, and we
384 selected a final height of 50 m to be high enough to focus on the overall 48-hour dynamics and
385 reduce the possible influence of surface topography. Contributions from air parcels extending
386 beyond 48 hours likely exist, but are outside of the regional scope of our study.

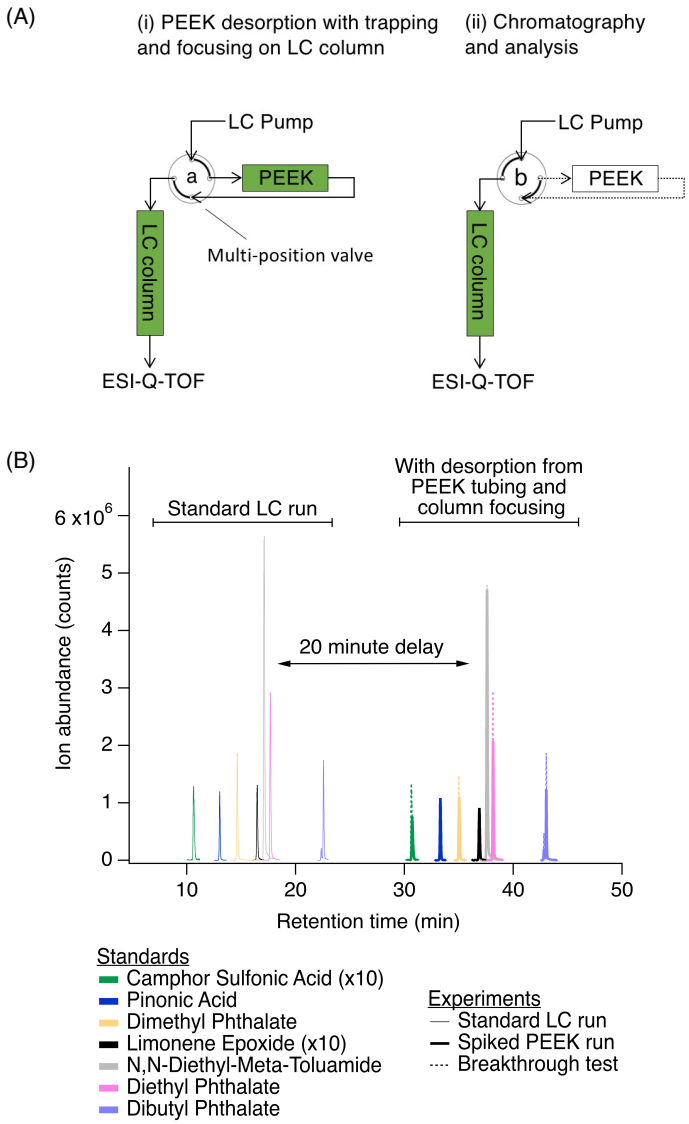

Figure 1. (A) Simplified analytical system setup for functionalized gas-phase compounds, showing (i) desorption from the PEEK collector and trapping on the LC column in order to focus analytes prior to chromatographic separation, and (ii) subsequent chromatographic separation and analysis (discussed in detail in Section S1). Green shading indicates active solvent flow through PEEK collector and/or LC column. A multi-position valve was switched from position "a" (panel (Ai)) to position "b" (panel (Aii)) to remove the PEEK collector from the flow path for chromatography and analysis. Table S1 describes the flow rates and solvents used in each of these steps. (B) Comparison of select peaks from a typical LC run (solid traces from 10-23 min) to that from a PEEK collector spiked with a standard (bold traces from 30-43 min) demonstrates desorption, trapping/focusing, and similar chromatography. Comparable results from a 2-hour breakthrough test at 2°C with 22 mL/min air flow are also shown (overlayed dotted traces from 30-43 min). Spiked PEEK and breakthrough tests were performed to validate this sampling and analysis methods, and are discussed further in Section S1. Test analytes were used across a range of functionality, with examples shown here and the full list in Table S2.

3. Results and Discussion

3.1. Characteristics of the Urban Regional Site

Backward trajectories for summertime and wintertime samples showed a strong urban influence. Summertime trajectories ranged from the northwest, west, and especially the southwest (i.e., New York City and other coastal metropolitan areas, similar to well-established and expected air flow patterns near the Long Island Sound). In contrast, trajectories were almost exclusively from the northwest in the winter (Figure S1). These air parcels brought a range of compounds from a mixture of anthropogenic, biogenic, and marine sources to the site, all with differences in gas- and particle-phase source profiles. However, due to the varied backward trajectories, dynamic variations in wind direction over the long duration filter samples (Figure S2), and a high degree of mixing over the Sound, our 8-hour samples are representative of mixed regional conditions in summer and winter, and are thus discussed in this context. Further detailed site characterization can be found in Section S2 and Figures S1-S3.

3.2. Summer and Winter Comparisons of Functionalized Organic Aerosols

3.2.1. Summertime composition and the influence of photochemistry and NO_x

During this period of active photochemistry, the observed distribution of particle-phase compounds in summertime samples spanned across the intermediate volatility (IVOC) to ultralow volatility organic compound (ULVOC) range, with a predominance of semivolatile (SVOC), low volatility (LVOC), and extremely low volatility organic compounds (ELVOC) as shown in Figure 2A as a function of compound class. To assess differences in summer and winter volatility distributions, we used individual molecular formulas and the Li et al. (2016) parameterization to estimate the saturation mass concentration ($\log(C_0)$) of each observed

compound (Li et al., 2016). Compounds were then classified into volatility bins following these definitions: VOC > $3*10^6$ μg/m^3; $3*10^6$ μg/m^3 > IVOC ≥ 300 μg/m^3; 300 μg/m^3 > SVOC ≥ 0.3 μg/m^3; 0.3 μg/m^3 > LVOC ≥ $3*10^{-5}$ μg/m^3; $3*10^{-5}$ μg/m^3 > ELVOC ≥ $3*10^{-9}$ μg/m^3; $3*10^{-9}$ μg/m^3 > ULVOC (Donahue et al., 2011; Schervish and Donahue, 2020).

Due to elevated summertime O_3 mixing ratios at the site (shown in Figure S3, 8-hour maximum mixing ratio in summer: 57 ± 20 ppb, vs. winter: 46 ± 5 ppb, including day and night sampling periods), O_3 may have influenced the photochemical processing of emitted volatile species, especially unsaturated biogenic VOCs which readily undergo ozonolysis due to their chemical structure. However, we did not observe a correlation between 8-hour maximum (or 8-hour average) O_3 mixing ratios with average particle-phase volatility (as saturation mass concentration), carbon number, or O/C (nor did we observe such relationships for gas-phase organic compounds). There were, however, weak relationships between NO_x mixing ratios and each of these particle-phase characteristics in the summer. While average NO_x mixing ratios were slightly lower during the summer (as shown in Figure S3, 2.3 ± 1.5 ppb in summer vs. 3.7 ± 2.7 ppb in winter), NO_x mixing ratios trended weakly with particle-phase O/C ($r \sim 0.45$), volatility (as saturation mass concentration, $r \sim 0.49$), and inversely with carbon number ($r \sim -0.56$) in summer.

While our correlations and conclusions are somewhat limited by the 8-hour filter sampling duration and the resulting highly regionally-mixed samples, one possible hypothesis is that the presence of NO_x could have promoted more fragmentation reactions in the gas-phase (Loza et al., 2014) that decreased average carbon number, and correspondingly increased volatility and O/C. In fact, we observed highly oxidized C_3-C_6 compounds in the gas-phase (from adsorbent tube measurements with GC-APCI (Section S2)) that were possibly products of these

fragmentation reactions of larger compounds. These trends of NO_x mixing ratios with O/C, volatility, and carbon number were not apparent for the observed complex mixture of gas-phase organic compounds. However, these highly oxidized gases may not have persisted in the gas-phase and could have been taken up by the condensed/aqueous phase due to their water solubility, where they would have instead contributed to the observed trends of NO_x with carbon number, volatility, and O/C in the particle-phase. We note that if there was significant uptake of gas-phase NO_z to the particle-phase, this may have in part contributed to the particle-phase correlations with NO_x given that the chemiluminescence NO_x analyzer used in this study is known to also respond to gas-phase NO_z (Dunlea et al., 2007).

Additionally, NO_x could have been involved in heterogeneous chemistry, promoting oxidation and/or nitrogen addition reactions, such as interaction with $NO_3^{\bullet}$ to yield organonitrates (Lim et al., 2016), formation and interaction with HONO to yield nitrophenols (Vidović et al., 2018), or other pathways.

3.2.2. Comparison to wintertime composition and the role of aqueous-phase chemistry

In the winter, these same relationships between NO_x and particle-phase characteristics were not observed. This is possibly due to the decreased role of photochemistry in the winter and the increased role of other competing physical and chemical processes, such as aqueous-phase chemistry. In the discussion of our results, we note that aqueous-phase chemistry is meant to be inclusive of aqueous processing in aerosols, in cloud water, and/or in fog water, all of which may have occurred upwind of the site during the 8 hour sampling periods under variable local and regional weather conditions.

In the winter, we observed a generally higher average saturation mass concentration (summer: $\log(C_0) = -3.7 \pm 3.9$ $\mu g/m^3$, vs. winter: $\log(C_0) = -0.7 \pm 4.0$ $\mu g/m^3$). We note that this comparison of saturation mass concentrations was performed at a reference temperature of 300 K, and we discuss the expected wintertime volatility shift below. The wintertime O/C was also slightly lower than summer (summer: O/C = 0.5 ± 0.4 vs. winter: O/C = 0.4 ± 0.4). In the winter, the observed chemical composition of the particle phase—both in terms of volatility and functional group distribution—suggests a relatively greater role for aqueous-phase processing. Our observations were similar to those made in past studies of higher volatility products from fragmentation reactions in the aqueous phase (e.g., Brege at al., where they observed that aged fog-water samples contained organic compounds with smaller carbon backbone structures than non-aqueous aged particles, and linked this difference to aqueous-phase fragmentation reactions, the uptake of smaller water-soluble gases to the aqueous-phase, and/or less oligomerization (Brege et al., 2018); Yu et al., which discussed the role of fragmentation in aging aqueous phenolic secondary organic aerosol (Yu et al., 2016); and Schurman et al., which discussed the role of fragmentation and evaporation in cloud water (Schurman et al., 2018)). Similarly, here we observed a shifted compound distribution that included smaller molecular weight and generally higher volatility particle-phase species in winter compared to summer, along with notably different functional group distribution, both of which could be attributed to aqueous chemistry.

We note that for direct comparison, volatility bins in Figure 2A-B were defined for the same reference temperature (i.e., 300 K, the average summertime sampling period temperature), though wintertime saturation mass concentrations for the observed compounds would shift approximately 2 orders of magnitude lower due to lower temperatures (i.e., 270 K). The dotted black line in Figure 2B shows the shift in bins expected at 270 K. In the winter, compounds

493 defined IVOCs or SVOCs at 300 K will expectedly exhibit a greater degree of partitioning to the
494 particle phase, though the effect of this temperature shift on partitioning was likely more
495 pronounced for the SVOCs than IVOCs (Table S4). Even when accounting for this shift, the
496 mean saturation mass concentration of wintertime samples was $\log(C_0) = -2.7 \pm 3.9$ $\mu g/m^3$,
497 which is still higher than the mean summertime saturation mass concentration of $\log(C_0) = 3.7 \pm$
498 3.9 $\mu g/m^3$ and thus still demonstrates a volatility difference between summer and winter, with
499 higher volatility species in winter. This shift is also reflected in the carbon number distribution
500 observed via the LC-ESI-MS/MS analysis of this sample set shown in Ditto et al., (2020), Figure
501 S5. In addition to this shift in molecular size and volatility, there was a distinct change functional
502 group composition from summer to winter, discussed below.
503 To assess the potential contribution of aqueous-phase chemistry, we also estimated
504 aerosol liquid water concentrations based on available data in Section S2.1. We estimated a
505 lower but still appreciable aerosol liquid water content in winter relative to summer, but with
506 fewer photochemical processes in winter along with generally cloudier/foggier local weather
507 (i.e., 44% of summer sampling periods with partly cloudy or cloudy weather conditions vs. 67%
508 of winter sampling periods, from Weather Underground archive), aqueous-phase processing
509 likely remains an important pathway. We note that the compounds discussed here could have
510 been formed locally or regionally, and thus the role of conditions at the site (aerosol liquid water,
511 cloud cover, fog cover) is just as important as the conditions in the surrounding upwind region.
512 As a result, it is challenging to pinpoint the exact contributions of aerosol liquid water, in-cloud,
513 or in-fog processing, and we consider that all three may be occurring upwind or near the site.
514 Furthermore, from MS/MS analysis, we observed functional groups that were possible
515 indicators of aqueous-phase processing, including the presence of nitrophenols during the winter,

516 which may have formed via dark aqueous-phase reactions with HONO (Vidović et al., 2018),
517 and relatively low contributions from carbonyls across seasons, possibly linked to carbonyl
518 hydrolysis (Ditto et al., 2020). Based on laboratory studies, the presence of azole functional
519 groups and other heterocyclic nitrogen species could also indicate aqueous phase processing, and
520 may be formed from small carbonyl precursors such as glyoxal (DeHaan et al., 2009; Grace et
521 al., 2019) and biacetyl (Grace et al., 2020) reacting with atmospheric ammonia or small amines.
522 Many of the N-only containing azoles observed here had similar substructures to those formed in
523 the aqueous-phase reactions of small carbonyls with ammonia/amines (DeHaan et al., 2009;
524 Grace et al., 2019). In addition, as discussed above, we observed many small gas-phase C_3-C_6
525 compounds at the site in the summer, which likely included multifunctional isoprene oxidation
526 products (e.g., glycoaldehyde, hydroxyacetone, and isomers); these potential precursors could
527 have reacted with atmospheric ammonia or species containing amino groups to form the
528 observed azole-containing reaction products. We observed more azoles during the summer (Ditto
529 et al., 2020), perhaps due to the increased prevalence of the C_3-C_6 precursors and overall
530 prominence of atmospheric water (e.g., aerosol liquid water, cloud water, fog water).
531 Lastly, the role of aqueous-phase chemistry in the region is further supported by prior
532 summertime observations at Brookhaven National Laboratory (on the opposite side of the Long
533 Island Sound), which examined a low-volatility oxygenated organic aerosol factor in the source
534 apportionment of aerosol mass spectrometry measurements, and showed a strong contribution
535 from carboxylic acids and other ELVOCs that were attributed to aqueous-phase processing
536 (Zhou et al., 2016).

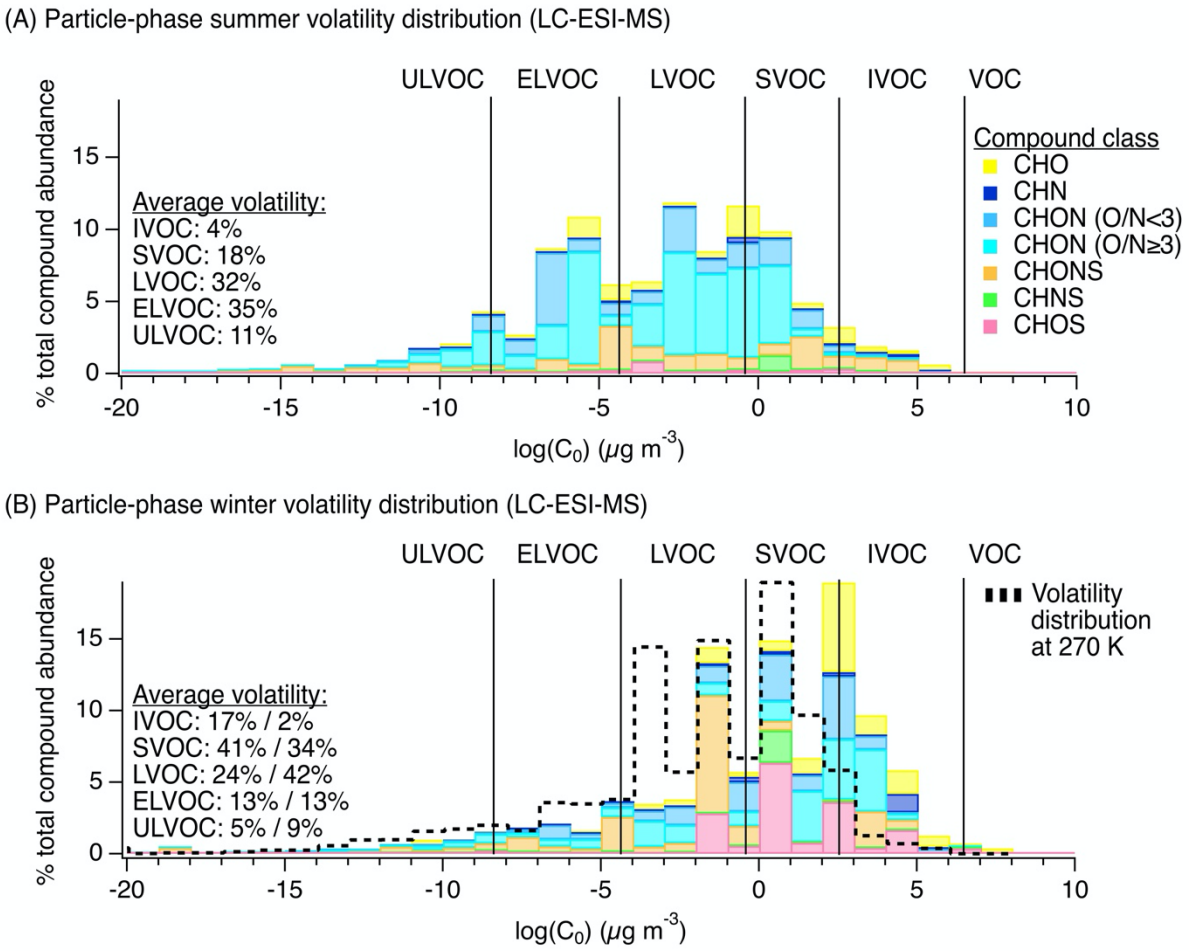

Figure 2. Chemical composition of particle-phase organic compound mixtures at the YCFS from LC-ESI-MS measurements. (A) and (B) show particle-phase volatility distributions by compound class in the summer (N=34) and winter (N=15), respectively, weighted by ion abundance. The same data tallied by occurrence are shown in Figure S4 for comparison. For direct comparison, volatility bins were defined for the same reference temperature in (A) and (B) (i.e., 300 K, the average summertime sampling period temperature), though wintertime saturation mass concentrations for the observed compounds would shift approximately 2 orders of magnitude lower due to lower temperatures (i.e., 270K). The dotted black line in (B) shows the shift in bins expected at 270 K, described further in Table S4. The average volatility distributions listed in (B) are shown at 300 K (%) followed by the estimate at 270 K (%).

3.2.3. Comparison to other sites using the same sampling and analytical methods

The distribution of compound classes observed at the YCFS was significantly different from observations at a range of field sites discussed in past studies (Figure 3), including a remote forested site (i.e., the PROPHET site in Northern Michigan), an urban inland site (i.e., near

553 downtown Atlanta) across two seasons, and in New York City (Ditto et al., 2018, 2019). We
554 perform a direct comparison to our past studies here, because the same sampling and analytical
555 methods were used, thus we can compare the distribution of ions observed without any biases
556 due to differences and uncertainties resulting from variations in sampling or ionization chemistry
557 between instruments. While a more detailed site-to-site comparison is outside the scope of this
558 work, the proximity of the YCFS to the ocean and thus the impact of marine emissions and over-
559 water chemistry likely contributed to the differences between the YCFS and inland locations. In
560 particular, at the YCFS, we observed notably smaller relative contributions from compounds
561 containing carbon, hydrogen, and oxygen (i.e., CHO, 11-16% of observed functionalized
562 compounds here vs. 34-50% at other sites), and the contributions from nitrogen-containing
563 particle-phase compounds at the YCFS were in stark contrast to other sites. Here, 85% of
564 compounds (by ion abundance) in summer and 68% of compounds in winter contained at least
565 one nitrogen atom, compared to 38-51% at the other previously studied sites (Figure 3). These
566 nitrogen-containing species were comprised of compounds with various reduced and oxidized
567 nitrogen-containing functional groups with varying oxygen-to-nitrogen ratios (O/N), which are
568 broadly classified and discussed below as compounds containing carbon, hydrogen, and nitrogen
569 (i.e., CHN), and compounds containing carbon, hydrogen, oxygen, and nitrogen (i.e., CHON
570 (O/N ratio < 3), and CHON (O/N ratio ≥ 3)). There were notably greater contributions at the site
571 from nitrogen-containing compounds that also contained at least one oxygen atom, including
572 CHON compounds with O/N < 3 (19-20% here vs. 10-15% at other sites), CHON compounds
573 with O/N ≥ 3 (24-44% here vs. 14-19% at other sites), as well as compounds containing oxygen,
574 nitrogen, and sulfur (i.e., CHONS, 20-21% here vs. 9-10% at other sites) (Ditto et al., 2018).

We note that while these measurements were of PM_{10} aerosols, the observations of high nitrogen content were not biased by the inclusion of larger, primary (possibly biological) particles. Quartz filter samples collected with a cascade impactor at the site during the summer and analyzed with the same LC-ESI-MS methods did not show any significant differences between any of these nitrogen-containing compound classes as a function of particle size, across particles ranging from 0.4 to 10 μm (i.e., 69%-71% of ion abundance for PM ≤ 2.2 μm and 69%-73% of ion abundance for PM ranging from 2.2-10 μm were nitrogen-containing species, summarized in Table S5). This is consistent with past studies which have demonstrated that amines, as one example of a prominent nitrogen-containing functional group, are ubiquitous in size-resolved aerosol samples in urban and rural locations (VandenBoer et al., 2011).

The prevalence of nitrogen-containing species at the YCFS is consistent with the study at Brookhaven National Laboratory discussed above, where a dedicated nitrogen-enriched aerosol mass spectrometry factor was identified, and contained prevalent signal from aliphatic amines and amides. However, in the Brookhaven study, the nitrogen-enriched factor was associated with industrial amine emissions that were enhanced during periods of south/southwestern backward trajectory influence, and that had correlations with tracers linked to industrial processes. In our study, there was no correlation between backward trajectory direction and the contribution of nitrogen-containing species. Also, wintertime air parcels arrived predominantly from directions other than south/southwest, suggesting that the nitrogen-containing species observed in our study were the result of mixed anthropogenic, biogenic, and marine precursors and their transformation products. This high nitrogen content at the YCFS, where aqueous-phase chemistry is expected to be important, is also consistent with the cloud water composition discussed in Zhao et al. (2013), which reported roughly 65% of detected ions in their cloud water samples to contain a nitrogen

atom, and the primary marine aerosol composition discussed in Wozniak et al. (2014), where 61% of their observed compounds contained nitrogen and 54% were CHON species.

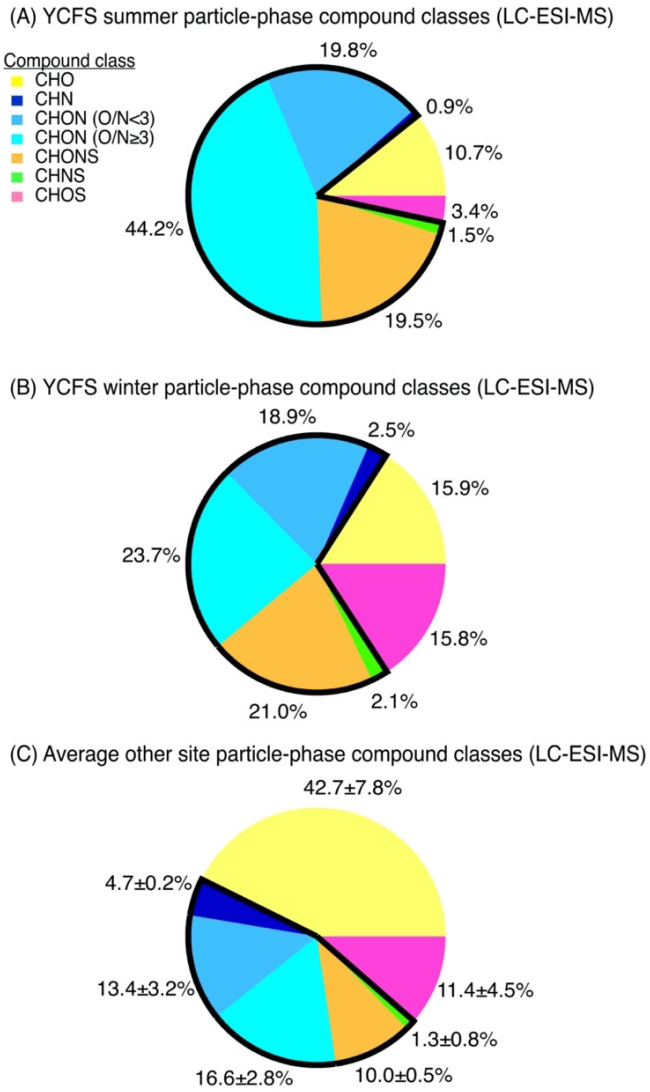

Figure 3. Particle-phase compound class distributions shown as fractions of total detected ion signal in the (A) summer and (B) winter at the YCFS, weighted by compound abundance, in contrast with (C) the average compound class distribution from previously studied forested, urban inland, and urban coastal sites. The sites selected for comparison in (C) were chosen because the same sampling and analysis methods were used. Nitrogen-containing compound class contributions are outlined in black, and are notably larger at the coastal site compared to other sites studied with these same filter collection and analysis methods. We note that while a significant fraction of species contained nitrogen, individual compounds contained 1-3 nitrogen atoms and the majority of the ion's molecular mass consisted of carbon and hydrogen atoms (mean N/C in summer: 0.13±0.1, mean N/C in winter: 0.22±0.19 for all N-containing ions). Note: CH and CHS species have poor ESI ionization efficiencies and are thus excluded here. Data tallied by occurrence are shown in Figure S5 for comparison.

3.3. Speciating Particle-Phase Multifunctional Nitrogen-Containing Compounds

The observed particle-phase species were highly functionalized, often multi-functional, and contained combinations of oxygen, nitrogen, and/or sulfur heteroatoms. Here, we discuss the functional groups present, broken up by the nitrogen-containing compound classes shown in Figures 2-3, with additional discussion of other relevant compound classes in Section S3.

3.3.1. CHN compounds

While nitrogen-containing compounds in general were very prominent at the site (Figure 3A-B), CHN compounds were relatively less abundant in these samples of functionalized organic aerosol. Particle-phase CHN compounds represented just 1% and 3% of observed functionalized organic aerosol abundance in summer and winter, respectively, which was similar to observations at other ambient sites (~5% CHN) (Ditto et al., 2018).

In the summertime LC-ESI-MS/MS measurements, CHN particle-phase compounds were comprised primarily of amines (72% of CHN species contained an amine group) and nitriles (28% of CHN species contained a nitrile group), as shown in Figure 4. In the winter, these compounds were nearly exclusively amines (present in 99% of CHN species). Amines have many primary land-based sources (e.g., biogenic emissions (Kieloaho et al., 2013), agricultural activity (Ge et al., 2011), emissions from decomposing organic matter (Ge et al., 2011; Sintermann and Neftel, 2015), biomass burning (Ge et al., 2011), emissions from port activity (Gaston et al., 2013), chemical products (Khare and Gentner, 2018), and vehicle exhaust (Sodeman et al., 2005)), but their presence on the coast could also indicate marine contributions. Amines have been detected both in bulk ocean water, the surface microlayer, and in sea spray aerosol, and their emissions and chemical transformations in the marine environment have been

636 the topic of many recent studies (e.g., Brean et al., 2021; Dall'Osto et al., 2019; Decesari et al.,
637 2020; Di Lorenzo et al., 2018; van Pinxteren et al., 2012, 2019; Quinn et al., 2015; Wu et al.,
638 2020). In the summer, biogenic and marine sources likely dominated the amine distribution,
639 while in the winter, anthropogenic amine sources likely became more important.
640 Recent studies have also evaluated amine phase partitioning or formation in cloud/flog
641 water (e.g., Chen et al., 2018; Youn et al., 2015), as well as condensed-phase or aqueous-phase
642 pathways that may transform emitted amines (e.g., Ge et al., 2016; Lim et al., 2019; Tao et al.,
643 2021). Interestingly, the observed amines at this site, as well as other reduced nitrogen groups
644 like nitriles, imines, and enamines, were not present exclusively in CHN species and thus were a
645 mix of both direct emissions and chemically processed compounds. Reduced nitrogen groups
646 were often paired with hydroxyl groups, carboxylic acids, carbonyls, ethers, and esters as part of
647 nitrogen and oxygen containing compounds with a range of O/N ratios. This is consistent with
648 other studies observing reduced-nitrogen contributions to CHON compound classes, such as
649 Zhao et al. (2013), LeClair et al. (2012), and Altieri et al (2009), discussed above. As such, we
650 discuss CHON species as a function of O/N ratio to focus on differences between less-
651 oxygenated (O/N < 3) and more-oxygenated (O/N ≥ 3, e.g., organonitrates) species, using a ratio
652 of 3 to distinguish between the two as informed by the O/N ratio of the organonitrate functional
653 group.
654
655 *3.3.2. CHON (O/N < 3) compounds*
656 CHON (O/N < 3) compounds were notably more important at this site than other sites,
657 representing 20% and 19% of observed functionalized organic aerosol abundance in summer and
658 winter, respectively (Figure 3A-B), compared to ~13% at other sites (from predominantly

summer measurements). These CHON compounds included some functional groups that contained both oxygen and nitrogen, such as amide groups (12% of this compound class's nitrogen content in summer, vs. 1% in winter, Figure 4) and nitro groups (15% of this nitrogen content in summer, vs. 6% in winter, Figure 4). However, most CHON (O/N < 3) compounds were comprised of a combination of nitrogen- *or* oxygen-containing groups, rather than a functional group containing both nitrogen and oxygen. This included large contributions from hydroxyls and ethers across both seasons, as well as important contributions from amines, isocyanates, and heterocyclic nitrogen, as shown in Ditto et al., 2020 (Figure 1). The presence of these functional groups in the winter could be indicative of wood burning emissions in the region, which has been observed in the wintertime in past ambient sampling in the Northeast U.S. (Sullivan et al., 2019). Isocyanates contributed notably to this compound class during the winter, which could similarly be linked to burning wood, other biomass, building materials (Leslie et al., 2019; Priestley et al., 2018; Roberts et al., 2014), or could be photochemically produced via the oxidation of amines and amides (Borduas et al., 2015; Leslie et al., 2019). Importantly, levoglucosan, a common biomass burning tracer, was observed across nearly all daytime and nighttime winter particle-phase samples (verified with an authentic standard), supporting the influence of biomass burning compounds at the site. Together, the overall high prevalence of reduced nitrogen at this site could be influenced by the mixing of aged biomass burning plumes with marine air, which is consistent with past observations of very high alkylamine concentrations in biomass burning particles that mixed with marine air prior to sampling (Di Lorenzo et al., 2018).

3.3.3. CHON (O/N ≥ 3) compounds

CHON (O/N ≥ 3) compounds were the dominant compound class in the observed summertime distribution and played an important role in the wintertime distribution as well, comprising 44% of observed functionalized organic aerosol abundance in summer vs. 24% in winter (Figure 3A-B). These contributions were far greater than the contributions of CHON (O/N ≥ 3) species at other sites, which typically ranged from 14-19% (predominantly from summertime measurement, Figure 3C).

Similar to CHON (O/N < 3), we observed some CHON (O/N ≥ 3) compounds with functional groups containing 3 oxygen atoms and 1 nitrogen atom, e.g., nitrophenols and organonitrates (Figure 4), but also contributions from nitrogen-only functional groups paired with oxygen-containing groups. Notably, in the summer, there were important contributions from amines (47% of this compound class's nitrogen content), imines (19%), organonitrates (10%), and azoles (16%) (Figure 4). In contrast, in the winter, nitrogen content in the CHON (O/N ≥ 3) compound class was dominated by I/SVOC nitrophenols, comprising 64% of the CHON (O/N ≥ 3) ion abundance.

NO_x mixing ratios were typically low in both summer and winter (2.3 ± 1.5 ppb in summer vs. 3.7 ± 2.7 ppb in winter), but were slightly higher during winter. In the winter, CHON (O/N ≥ 3) compounds showed a weak positive relationship with NO_x mixing ratios ($r \sim 0.58$) and a stronger correlation with NO mixing ratios ($r \sim 0.81$). This relationship between CHON (O/N ≥ 3) and NO (and NO_x) suggests that many of these oxidized nitrogen species were products of NO_x-related chemistry (i.e., NO_z compounds). The enhancements in nitrophenols serves as one example of this, as NO mixing ratios also correlated with the contribution of nitrophenols in the winter ($r \sim 0.69$).

In past work, we discussed nitrophenol nighttime enhancements during winter, and noted their reported aqueous formation pathways mentioned in prior laboratory studies (Ditto et al., 2020). Here, we demonstrate that nitrophenols were important contributors to the CHON (O/N ≥ 3) compound class, and highlight their role as examples of NO_z due to their possible formation via dark aqueous-phase nitration pathways of oxygenated aromatics with ambient nitrous acid (HONO) (Vidović et al., 2018). While nitrophenols may have other sources (e.g., diesel exhaust), our observations of a clear nighttime enhancement during the winter suggest that these functional groups were most likely formed by secondary chemistry related to NO_x oxidation, as this field site was removed from major roadways. Our wintertime observations suggest that HONO could have been derived from local wood burning, and could have reacted away as the smoke plume aged to form stable products like nitrophenols, similar to HONO transformation chemistry into other forms of oxidized nitrogen (e.g., particulate nitrates, PANs, organic nitrates) that has recently been observed in wildfire smoke (Juncosa Calahorrano et al., 2021).

Furthermore, the correlation between NO and CHON (O/N ≥ 3) could also be influenced by the daytime formation of organonitrates via reaction with $OH^{\bullet}$ and NO (i.e., $RO_2^{\bullet}$ + NO) (Liebmann et al., 2019; Ng et al., 2017; Perring et al., 2013; Takeuchi and Ng, 2018), though organonitrates contributed to a smaller fraction of CHON (O/N ≥ 3) species (i.e., 10% of this compound class's nitrogen content across seasons).

3.3.4. Overall contributions of reduced and oxidized nitrogen groups

In the summer and winter, contributions from reduced nitrogen groups (e.g., groups shown in black/grey in Figure 4) rivaled that of oxidized nitrogen groups in CHON compounds across a range of O/N ratios. In the summer, reduced nitrogen groups contributed to 50% of all

detected CHON (O/N < 3) compounds by ion abundance, while in the winter they contributed 47% (Figure 4). For CHON compounds with O/N ≥ 3, reduced nitrogen groups contributed to 68% of compound ion abundance in the summer (possibly related to marine influences (Wozniak et al., 2014)), while in the winter they contributed just 13%. Interestingly, 90% of the dominant reduced nitrogen functional groups observed (amines and imines) were present in acyclic rather than cyclic structures, which may have been the result of either direct emissions or formation via reactions with ammonia or other small amines.

In contrast, possible NO_z products (e.g., groups shown in blue in Figure 4) were present in 18% and 7% of CHON (O/N < 3) compounds in the summer and winter, respectively. For CHON (O/N ≥ 3) compounds, they were present in 18% and 86% in the summer and winter, respectively, with the latter wintertime increase in oxidized N-groups largely driven by the presence of nitrophenols at night (Ditto et al., 2020). The remaining fraction of nitrogen-containing groups also contained oxygen, but with a reduced nitrogen atom (e.g., amide, isocyanate, nitrogen/oxygen-containing azole, shown in brown in Figure 4). We note that CHONS compounds also represented a sizable fraction of observed organic nitrogen (Figure 3), and contained a mix of reduced and oxidized functional groups (Section S3 and Figures S7-8).

The importance of reduced nitrogen functional groups in CHON compounds highlights that not all oxygen- and nitrogen-containing species in the CHON (O/N ≥ 3) compound class were NO_z, despite their apparent molecular formulas and the observed correlation observed between CHON (O/N ≥ 3) species with NO and NO_x mixing ratios. For instance, many of the observed reduced nitrogen-containing functional groups co-occurred with several oxygen-containing groups like hydroxyls, carboxylic acids, esters, ethers, and carbonyls, and thus had

molecular formulas with O/N ≥ 3, which could incorrectly be assumed to be an organonitrate or similar structure based on molecular formula alone.

We note that the relative distribution of reduced and oxidized nitrogen-containing groups shown here is subject to sampling and ionization conditions. While the electrospray ionization source used for the particle-phase analysis discussed here effectively ionized these nitrogen-containing groups, their relative sensitivity may differ because many of these functional groups were present in multifunctional compounds whose other features may also contribute to ionization behavior. Also, other aspects of the sample collection and extraction process could cause variability in observed signal (e.g., PM size cut, organonitrate stability over long duration samples). Thus, we emphasize that the observed relative abundances here are valuable because they suggest that fully reduced nitrogen-containing groups are important contributors to multifunctional CHON species, but their exact mass contributions remain uncertain.

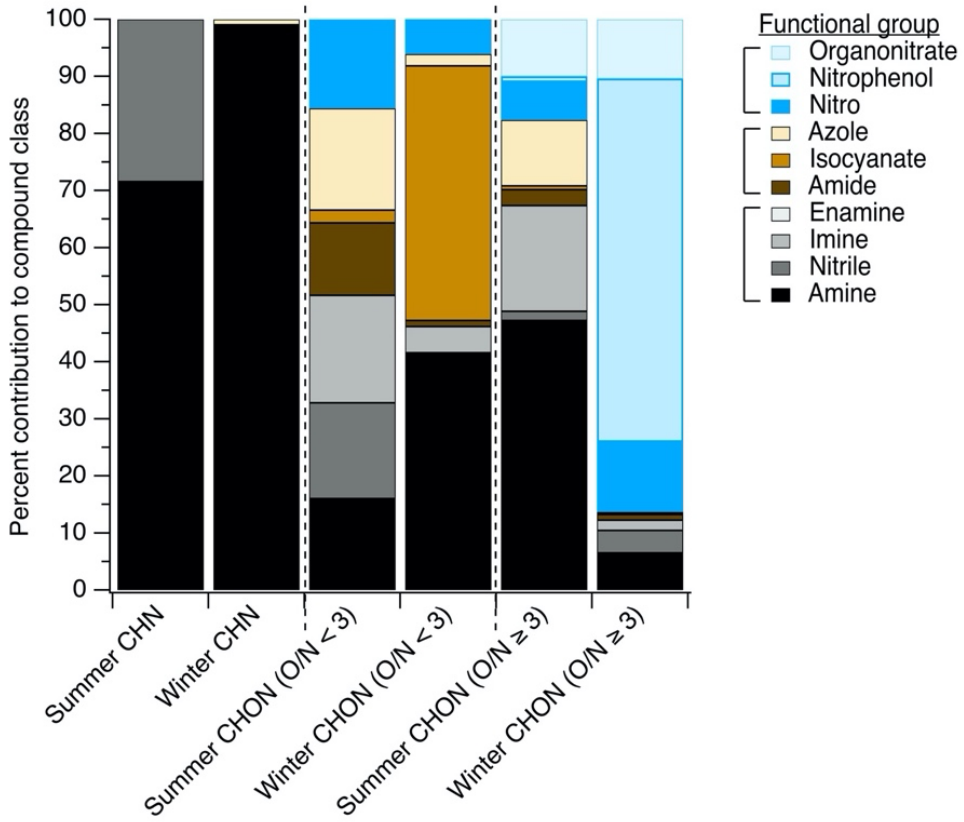

762

763 **Figure 4.** The distribution of functional groups in particle-phase nitrogen-containing compounds
764 measured via LC-ESI-MS/MS. The breakdown of CHN, CHON (O/N < 3), and CHON (O/N ≥
765 3) compounds is shown as a function of contributions of each functional group to ion abundance,
766 with possible NO_z species shown in blue shades, fully-reduced nitrogen-containing groups
767 shown in black/grey shades, and groups containing both oxygen and nitrogen where the nitrogen
768 atom itself is not oxidized shown in brown shades. The same data tallied by occurrence are
769 shown in Figure S6 for comparison. Figures S7 and S8 show the functional group distribution for
770 CHNS and CHONS compound classes tallied by abundance and by occurrence, respectively.
771
772
773 3.4. Probing Possible Nitrogen-Containing Gas-Phase Precursors to Observed Nitrogen-

774 Containing Particles with Adsorptive Sampling and LC-ESI-MS

775 The particle-phase volatility distribution in the winter ranged from IVOC-ULVOC. Of
776 the observed compounds in winter, 68% contained nitrogen; these likely included contributions
777 from functionalized gas-phase precursors and likely were influenced by the active multiphase
778 partitioning of these precursors, and their gas- or particle-phase reaction products, with changes

779 in organic aerosol loading, atmospheric liquid water concentrations, and temperature (Donahue
780 et al., 2011; Ervens et al., 2011). This emphasizes the need to measure a broader range of these
781 functionalized gas-phase compounds, which have known limitations with GC transmission, but
782 represent uncertain and important-to-measure SOA precursors.

783 However, despite evidence of higher volatility particle-phase compounds with diverse
784 nitrogen-containing functionalities that could dynamically partition between phases (Figure 2A-
785 B), the observed compound class distribution from gas-phase adsorbent tube measurements
786 analyzed via GC-APCI-MS was dominated by hydrocarbons (i.e., CH, 24% of detected ion
787 abundance in summer vs. 18% in winter) and oxygenates (i.e., CHO, 66% in summer vs. 69% in
788 winter) (Figure S10-11). These gas-phase species appeared to be lightly functionalized
789 oxygenates (average O/C: 0.12 ± 0.13), showing minimal contributions from nitrogen (or sulfur)
790 heteroatoms; only 9% of detected ion abundance from gas-phase adsorbent tubes in summer and
791 11% in winter contained a nitrogen heteroatom. This is likely due to measurement limitations;
792 while GC-APCI techniques are extremely well-suited for the analysis of less functionalized
793 organic compounds from both instrument transmission and ionization efficiency perspectives,
794 these techniques are not as effective for more polar, more functionalized, more thermally-labile,
795 or otherwise less-GC-amenable species. Thus, to examine a broader range of functionalized gas-
796 phase compounds, we used an offline adsorptive sampling method on cooled PEEK tubing
797 collectors and inline mobile phase desorption for LC-ESI-MS analysis (Figure 1). CH and CHS
798 compound classes were excluded from this gas-phase LC-ESI-MS analysis due to their poor ESI
799 ionization efficiency.

800 Due to variations in trapping and desorption effectiveness (Section S1), this method was
801 not intended to be used as a quantitative measurement of concentration, but rather a relative

assessment of the distribution of nitrogen-containing gas-phase organic compounds. The variation between analytes in breakthrough testing does not influence our conclusions about the overall prevalence of observed gas-phase organic nitrogen. In laboratory tests, gas-phase sample collection, inline desorption to the mobile phase, trapping on the LC column, and chromatographic separation performed well. We observed limited breakthrough for most analytes during sampling, effective focusing prior to LC analysis, and similar separations for spiked collectors and breakthrough tests compared to standard LC runs (Figure 1B).

Results from the application of this new method at the YCFS revealed a wide range of compounds with oxygen-, nitrogen-, and/or sulfur-containing functionality (Figure 5) that existed at a lower average saturation mass concentration than the adsorbent tube methods during winter, with a $\log(C_0)$ of 3.5 ± 3.1 $\mu g/m^3$ for adsorbent tubes analyzed with GC-APCI-MS compared to 1.9 ± 2.1 $\mu g/m^3$ for functionalized gases observed via LC-ESI-MS. This decrease in volatility corresponded to an increase in the average O/C ratio of these functionalized gases to 0.24 ± 0.24, which can partly be attributed to LC-ESI's poor ionization of CH compounds and to the collection system's design (targeting heteroatom-containing species and not higher volatility hydrocarbons). This may be a lower limit of O/C among functionalized compounds, as during testing with a mixture of standards, we often observed poor retention of high O/C sugars like xylitol and mannose on the LC analytical column (Table S2).

The gas-phase LC-ESI-MS data provide a valuable comparison to the wintertime particle-phase samples analyzed using the same instrument. These particle-phase samples had major contributions from CHO, CHON ($O/N < 3$ and $O/N \geq 3$), CHONS, and CHOS compound classes (Figure 3B). While not collected concurrently, the functionalized gas-phase samples in winter had similar contributions from CHO (20%) and CHON ($O/N \geq 3$) compounds (16%),

relatively more CHN (11%) and CHON (O/N < 3) (46%) compounds, and fewer CHONS (2.7%) and CHOS (4.4%) compounds (Figure 5A). The prevalence of gas-phase CHN, CHON (O/N < 3), and CHON (O/N ≥ 3) is of particular interest given the abundance of CHON compounds observed in the particle phase, and the potential of these gases to partition to the particle-phase and/or act as reactive precursors to other oxidized nitrogen-containing species.

The presence of these nitrogen-containing compounds in the gas-phase also suggests that these compound classes observed in the particle-phase at least partly originated in the gas-phase and partitioned, rather than formed exclusively as a result of particle-phase chemistry. These species could have also formed in the particle-phase and partitioned to the gas-phase with or without condensed-phase fragmentation (discussed above). In either scenario, these nitrogen-containing compounds likely actively partitioned between phases due to their volatility (e.g., I/SVOCs shown in Figure 5A). Also, their polarity and high Henry's Law coefficients (relative to non-functionalized hydrocarbons (Sander, 2015)) suggests that these compounds could have been readily taken up by the aqueous phase. To check that these compounds were indeed gas-phase species under ambient conditions, we predicted the saturation mass concentration for individual compounds using individual ion formulas and estimated their gas-particle partitioning to a pre-existing condensed phase. While the range of compounds in Figure 5A can be expected to dynamically partition, the results confirm that the overall suite of observed compounds would have predominately existed as gases, with on average ~80% of observed ion abundance predicted to equilibrate to the gas-phase across compound classes (Figure S12-13).

Of all the gas-phase species observed with at least one nitrogen atom (i.e., CHN, CHON, CHONS, CHNS), collected in winter, we note that 78% of these compounds had an O/N ratio of less than 3 (Figure 5B), indicating that most of these gas-phase species were not organonitrates,

nitrophenols, or other similar structures. This is similar to our particle-phase wintertime results, which showed important contributions from reduced nitrogen-containing groups paired with oxygen-containing groups in CHON (O/N < 3) compounds. Notably, we observed an 11% contribution of gas-phase CHN species with this gas-phase LC-ESI-MS method (Figure 5A), in contrast to 2% CHN in the wintertime particle-phase samples (Figure 3). In the winter particle-phase samples, most CHN compounds contained amines (discussed above), and thus we postulate that these functionalized gas-phase CHN species were possibly also amines that acted as precursors to observed nitrogen-containing particle-phase compounds following oxidation and partitioning (or vice versa).

The substantial contribution from CHON with O/N < 3 (46%) to the functionalized gas-phase samples could be linked to less photochemical processing of CHON compounds relative to the particle phase and/or the emissions/oxidation of CHN or CHON compounds. Moreover, in the particle-phase, we observed a weak negative relationship between CHN contribution and hydroxyl group prevalence in summertime measurements (r~ -0.57), which may support the transformation of CHN to CHON compounds via the formation of hydroxyl-containing species. The elemental ratio distribution of these functionalized gases is summarized in Figure S14 and Table S6.

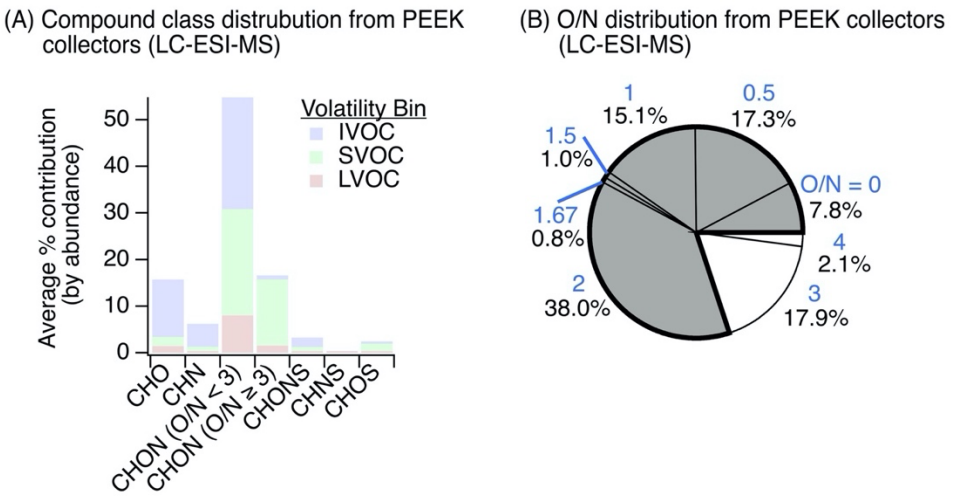

Figure 5. Observations of gas-phase nitrogen-containing compounds. (A) The distribution of functionalized gases observed via sampling on PEEK collectors (N = 6) and inline mobile phase desorption with non-targeted LC-ESI-MS analysis contained a diversity of oxygen-, nitrogen-, and/or sulfur-containing compounds in the IVOC-LVOC range (volatility assignment and grouping was the same as discussed in Figure 2 at a reference temperature of 300 K for intercomparison). While we cannot rule out gas-phase LVOC contributions from evaporation off of the upstream particle filter, LVOC contributions were limited (~12%). (B) Oxygen-to-nitrogen (O/N) ratio distribution of observed gas-phase nitrogen-containing species where O/N ratios < 3 are colored grey and O/N ratios ≥ 3 are colored white (blue text above each percentage signifies the O/N ratio). The same data, tallied by occurrence, are shown in Figure S9 for comparison.

4. Conclusions and Opportunities for Future Research

Together, these results suggest that a mix of direct emissions and chemical processes during summer and winter in the Long Island Sound region resulted in a diverse mixture of multifunctional gases and particles, where more than two-thirds of observed particle-phase compounds contained at least one nitrogen atom.

The observed nitrogen-containing functional groups existed across a range of fully reduced (e.g., amines, imines) to oxidized (e.g., nitro, organonitrate) structures. These fully reduced nitrogen functional groups were prevalent across all nitrogen-containing compound classes, including CHON species, and we highlight their importance as contributors to these multifunctional compounds beyond typical NO_z-type compounds that are commonly studied

using online mass spectrometers and share similar CHON molecular formulas. For instance, these gas- and particle-phase measurements of nitrogen-containing compounds are complementary to the measurements of these species made by chemical ionization mass spectrometers (CIMS) or by proton transfer reaction mass spectrometers (PTR-MS), whose ionization mechanisms can be tuned for sensitivity towards functionalized compounds of interest (Riva et al., 2019). While online mass spectrometers excel at high time resolution measurements that capture dynamic chemical processes in the atmosphere, their mass resolution is typically lower and they normally do not utilize separations, so they largely depend on parent ion mass-to-charge ratios to assign molecular formulas without structural attribution. The offline methods used here cannot match the time resolution of online techniques. However, the use of chromatography to separate isomers, longer sampling times to increase sensitivity toward a greater range of compounds, and the use of higher resolution mass spectrometers with MS/MS capabilities allow for improved compound identification and determination of functional group distribution at the molecular level. This enables us to distinguish between true NO_z species and those that contain combinations of nitrogen and oxygen but are not NO_x oxidation products. Thus, both these online and offline methods should be employed together to differentiate a wider range of nitrogen-containing species and to achieve both temporal and chemical resolution.

As discussed throughout this work, the Long Island Sound region is affected by a mixture of anthropogenic, biogenic, and marine sources, all of which contain known emitters of organic nitrogen. Understanding the combined effect of these individual sources and their chemical transformations will be important in regions like the Long Island Sound, where a significant degree of mixing occurs over the Sound before air parcels arrive inland. For example, past work has noted extremely high contributions from alkylamines in biomass burning-influenced air

911 mixed with marine air (Di Lorenzo et al., 2018). Similar enhancements could be expected when
912 mixing other prominent sources of amines with marine air, such as in the aging urban outflow
913 from the Central Atlantic and Northeast U.S., which may be transported up the coast and impact
914 states in the surrounding region.

915 As with any ambient site, these mixed emissions are chemically processed in the
916 atmosphere via a multitude of pathways. Here, we observed evidence of photochemical and
917 aqueous processes occurring in both seasons, but in the winter we observed various mixture-wide
918 trends that suggested an enhanced role for aqueous-phase processing. These observations
919 included higher overall particle-phase volatility and smaller carbon backbone sizes, which may
920 indicate a more important role for aqueous-phase fragmentation reactions or aqueous uptake of
921 water soluble gases (Brege et al., 2018). We also observed key marker functional groups that
922 may be formed via aqueous phase chemistry (e.g., nitrophenols, azoles). The role of aqueous-
923 phase chemistry and aqueous-phase uptake of gases is increasingly studied in laboratory and
924 ambient contexts (Herrmann et al., 2015), and such chemistry should further examined especially
925 in coastal and other humid regions.

926 For example, the aqueous-phase processing of atmospherically relevant nitrogen-
927 containing species is particularly important to understand in ambient air due to the potential of
928 brown carbon formation, which has significant impacts on climate forcing (Laskin et al., 2015).
929 The role of ammonia and amines reacting with carbonyls is of interest for this type of chemistry
930 (e.g., DeHaan et al., 2009; Grace et al., 2020; McNeill, 2015; Sareen et al., 2010) and should
931 continue to be explored, particularly in coastal settings where concentrations of small gas-phase
932 amines may be high due to their marine sources. As discussed above, our ambient observations
933 of azoles could be indicative of such chemistry, and should be explored in future comparisons of

ambient and laboratory-generated species. Also, we observed a significant contribution from nitrophenols at our site, and while they are not formed by this same chemistry, they represent another important form of light absorbing nitrogen-containing organic mass in the atmosphere (Hems and Abbatt, 2018). Finally, many of the nitrogen-containing functional groups observed in this work may be susceptible to hydrolysis, so the balance between hydrolysis and other aqueous pathways is important to consider and understand for appropriate representation of nitrogen-containing compounds in models for both aqueous aerosol and in-cloud/fog chemistry.

As another example, the greater prevalence overall higher volatility species observed in the winter particle-phase samples suggested possible dynamic partitioning or aqueous uptake of lighter gas-phase compounds; to explore the composition of these lighter gas-phase compounds that could exist as I/SVOCs and thus participate in phase partitioning, we supplemented our particle-phase analyses with a novel approach for investigating functionalized gases with LC-ESI-MS. Further investigation of these nitrogen-containing gases will facilitate new understanding of their gas-particle partitioning in the presence of atmospheric water and organic condensed species, and measurements across dynamic conditions will help elucidate the relative importance of both processes. For these types of measurements, further design iterations of the PEEK sampling system for functionalized gases and additional functionalized gas-phase samples for LC-ESI-MS analysis could be pursued. Concurrent high volume filter samples could be collected for direct comparison to the particle-phase, which was not possible in this study due to insufficient mass loading on the upstream filter during the short duration functionalized gas sample (i.e., 2 hours). Concurrent PEEK samples could also be collected for MS/MS analysis.

In all, combinations of online and offline mass spectrometry to obtain temporal and chemical detail, further ambient observations of major organic nitrogen sources, a better

understanding of the aqueous processing of nitrogen-containing compounds, and improved characterization of their gas-particle partitioning in the presence of atmospheric water will together allow for a more accurate representation of nitrogen-containing organic compounds in emission inventories and models, and enhance our ability to predict their impacts on atmospheric composition, human health, and climate.

Author contributions: J.C.D. and D.R.G. planned the field sampling and study. J.C.D. collected and analyzed field samples, and performed PEEK sampling and inline LC method development. J.M. performed inline LC method development. J.C.D. and D.R.G. wrote the manuscript with contributions from all co-authors.

Data availability: Available upon request to Drew R. Gentner (drew.gentner@yale.edu).

Competing interests: The authors declare that they have no substantive conflicts of interest but acknowledge that D.R.G. is an associate editor with *Atmospheric Chemistry and Physics*.

Acknowledgements: We acknowledge support from the National Science Foundation (AGS1764126) and the Yale Natural Lands Program. J.M. thanks the Goodyear Tire & Rubber Company and the Grumman Fellowship. We also acknowledge GERSTEL for their collaboration with the thermal desorption unit used here. We thank David Wheeler at the New York Department of Environmental Conservation, Pete Babich and Adam Augustine at the Connecticut Department of Energy and Environmental Protection, Luke Valin at the Environmental Protection Agency, and Jordan Peccia at Yale for use of sampling equipment, as well as Paul Miller (NESCAUM) for organizing the LISTOS project. We also thank Richard

Boardman and the Yale Peabody Museum for enabling us to set up and collect samples at the YCFS site, and acknowledge the help of Yale Peabody Museum EVOLUTIONS interns: Amir Bond, Ethan Weed, Paula Mock, and Aurea Orencia. We thank Trevor VandenBoer and Barbara Ervens for helpful feedback on the draft manuscript. Finally, we acknowledge the NOAA Air Resources Laboratory (ARL) for the provision of the HYSPLIT transport and dispersion model.

References

Altieri, K. E., Turpin, B. J. and Seitzinger, S. P.: Composition of dissolved organic nitrogen in continental precipitation investigated by ultra-high resolution FT-ICR mass spectrometry, Environ. Sci. Technol., 43(18), 6950–6955, doi:10.1021/es9007849, 2009.

Boone, E. J., Laskin, A., Laskin, J., Wirth, C., Shepson, P. B., Stirm, B. H. and Pratt, K. a.: Aqueous Processing of Atmospheric Organic Particles in Cloud Water Collected via Aircraft Sampling, Environ. Sci. Technol., 150611113115005, doi:10.1021/acs.est.5b01639, 2015.

Borduas, N., Da Silva, G., Murphy, J. G. and Abbatt, J. P. D.: Experimental and theoretical understanding of the gas phase oxidation of atmospheric amides with OH radicals: Kinetics, products, and mechanisms, J. Phys. Chem. A, 119(19), 4298–4308, doi:10.1021/jp503759f, 2015.

Brean, J., Dall'Osto, M., Simó, R., Shi, Z., Beddows, D. C. S. and Harrison, R. M.: Open ocean and coastal new particle formation from sulfuric acid and amines around the Antarctic Peninsula, Nat. Geosci., 14(6), 383–388, doi:10.1038/s41561-021-00751-y, 2021.

Brege, M., Paglione, M., Gilardoni, S., Decesari, S., Facchini, M. C. and Mazzoleni, L. R.: Molecular insights on aging and aqueous-phase processing from ambient biomass burning emissions-influenced Po Valley fog and aerosol, Atmos. Chem. Phys., 18(17), 13197–13214, doi:10.5194/acp-18-13197-2018, 2018.

Chen, C. L., Chen, S., Russell, L. M., Liu, J., Price, D. J., Betha, R., Sanchez, K. J., Lee, A. K. Y., Williams, L., Collier, S. C., Zhang, Q., Kumar, A., Kleeman, M. J., Zhang, X. and Cappa, C. D.: Organic Aerosol Particle Chemical Properties Associated With Residential Burning and Fog in Wintertime San Joaquin Valley (Fresno) and With Vehicle and Firework Emissions in Summertime South Coast Air Basin (Fontana), J. Geophys. Res. Atmos., 123(18), 10707–10731, doi:10.1029/2018JD028374, 2018.

Cleveland, W. S., Kleiner, B., McRae, J. E. and Warner, J. L.: Photochemical air pollution: Transport from the New York City area into Connecticut and Massachusetts, Science., 191(4223), 179–181, doi:10.1126/science.1246603, 1976.

Dall'Osto, M., Airs, R. L., Beale, R., Cree, C., Fitzsimons, M. F., Beddows, D., Harrison, R. M., Ceburnis, D., O'Dowd, C., Rinaldi, M., Paglione, M., Nenes, A., Decesari, S. and Simó, R.: Simultaneous Detection of Alkylamines in the Surface Ocean and Atmosphere of the Antarctic Sympagic Environment, ACS Earth Sp. Chem., 3(5), 854–862, doi:10.1021/acsearthspacechem.9b00028, 2019.

Decesari, S., Paglione, M., Rinaldi, M., Dall'osto, M., Simó, R., Zanca, N., Volpi, F., Cristina Facchini, M., Hoffmann, T., Götz, S., Johannes Kampf, C., O'Dowd, C., Ceburnis, D., Ovadnevaite, J. and Tagliavini, E.: Shipborne measurements of Antarctic submicron organic aerosols: An NMR perspective linking multiple sources and bioregions, Atmos. Chem. Phys., 20(7), 4193–4207, doi:10.5194/acp-20-4193-2020, 2020.

DeHaan, D. O., Corrigan, A. L., Smith, K. W., Stroik, D. R., Turley, J. J., Lee, F. E., Tolbert, M. A., Jimenez, J. L., Cordova, K. E., Ferrell, G. R., Haan, D. O. De, Corrigan, A. L., Smith, K. W., Stroik, D. R., Turley, J. J., Lee, F. E.,

Tolbert, M. A., Jimenez, J. L., Cordova, K. E. and Ferrell, G. R.: Secondary organic aerosol-forming reactions of glyoxal with amino acids, Environ. Sci. Technol., 43(8), 2818–2824, doi:10.1021/es803534f, 2009.

Di, Q., Wang, Y., Zanobetti, A., Wang, Y., Koutrakis, P., Choirat, C., Dominici, F. and Schwartz, J. D.: Air pollution and mortality in the medicare population, N. Engl. J. Med., 376(26), 2513–2522, doi:10.1056/NEJMoa1702747, 2017.

Ditto, J. C., Barnes, E. B., Khare, P., Takeuchi, M., Joo, T., Bui, A. A. T., Lee-Taylor, J., Eris, G., Chen, Y., Aumont, B., Jimenez, J. L., Ng, N. L., Griffin, R. J. and Gentner, D. R.: An omnipresent diversity and variability in the chemical composition of atmospheric functionalized organic aerosol, Commun. Chem., 1(1), 75, doi:10.1038/s42004-018-0074-3, 2018.

Ditto, J. C., Joo, T., Khare, P., Sheu, R., Takeuchi, M., Chen, Y., Xu, W., Bui, A. A. T., Sun, Y., Ng, N. L. and Gentner, D. R.: Effects of Molecular-Level Compositional Variability in Organic Aerosol on Phase State and Thermodynamic Mixing Behavior, Environ. Sci. Technol., 53(22), 13009–13018, doi:10.1021/acs.est.9b02664, 2019.

Ditto, J. C., Joo, T., Slade, J. H., Shepson, P. B., Ng, N. L. and Gentner, D. R.: Nontargeted Tandem Mass Spectrometry Analysis Reveals Diversity and Variability in Aerosol Functional Groups across Multiple Sites, Seasons, and Times of Day, Environ. Sci. Technol. Lett., 7(2), 60–69, doi:10.1021/acs.estlett.9b00702, 2020.

Ditto, J. C., He, M., Hass-Mitchell, T. N., Moussa, S. G., Hayden, K., Li, S.-M., Liggio, J., Leithead, A., Lee, P., Wheeler, M. J., Wentzell, J. J. B. and Gentner, D. R.: Atmospheric Evolution of Emissions from a Boreal Forest Fire: The Formation of Highly-Functionalized Oxygen-, Nitrogen-, and Sulfur-Containing Compounds, Atmos. Chem. Phys., 21, 255–267, 2021.

Donahue, N. M., Epstein, S. A., Pandis, S. N. and Robinson, A. L.: A two-dimensional volatility basis set: 1. organic-aerosol mixing thermodynamics, Atmos. Chem. Phys., 11(7), 3303–3318, doi:10.5194/acp-11-3303-2011, 2011.

Dührkop, K., Shen, H., Meusel, M., Rousu, J. and Böcker, S.: Searching molecular structure databases with tandem mass spectra using CSI:FingerID, Proc. Natl. Acad. Sci., 112(41), 12580–12585, doi:10.1073/pnas.1509788112, 2015.

Dührkop, K., Fleischauer, M., Ludwig, M., Aksenov, A. A., Melnik, A. V., Meusel, M., Dorrestein, P. C., Rousu, J. and Böcker, S.: SIRIUS 4: a rapid tool for turning tandem mass spectra into metabolite structure information, Nat. Methods, 16(4), 299–302, doi:10.1038/s41592-019-0344-8, 2019.

Dunlea, E. J., Herndon, S. C., Nelson, D. D., Volkamer, R. M., San Martini, F., Sheehy, P. M., Zahniser, M. S., Shorter, J. H., Wormhoudt, J. C., Lamb, B. K., Allwine, E. J., Gaffney, J. S., Marley, N. A., Grutter, M., Marquez, C., Blanco, S., Cardenas, B., Retama, A., Ramos Villegas, C. R., Kolb, C. E., Molina, L. T. and Molina, M. J.: Evaluation of nitrogen dioxide chemiluminescence monitors in a polluted urban environment, Atmos. Chem. Phys., 7(10), 2691–2704, doi:10.5194/acp-7-2691-2007, 2007.

Ervens, B., Turpin, B. J. and Weber, R. J.: Secondary organic aerosol formation in cloud droplets and aqueous particles (aqSOA): A review of laboratory, field and model studies, Atmos. Chem. Phys., 11(21), 11069–11102, doi:10.5194/acp-11-11069-2011, 2011.

Gaston, C. J., Quinn, P. K., Bates, T. S., Gilman, J. B., Bon, D. M., Kuster, W. C. and Prather, K. A.: The impact of shipping, agricultural, and urban emissions on single particle chemistry observed aboard the R/V Atlantis during CalNex, J. Geophys. Res. Atmos., 118(10), 5003–5017, doi:10.1002/jgrd.50427, 2013.

Ge, X., Wexler, A. S. and Clegg, S. L.: Atmospheric amines - Part I. A review, Atmos. Environ., 45(3), 524–546, doi:10.1016/j.atmosenv.2010.10.012, 2011.

Ge, Y., Liu, Y., Chu, B., He, H., Chen, T., Wang, S., Wei, W. and Cheng, S.: Ozonolysis of Trimethylamine Exchanged with Typical Ammonium Salts in the Particle Phase, Environ. Sci. Technol., 50(20), 11076–11084,

doi:10.1021/acs.est.6b04375, 2016.

Gioda, A., Reyes-Rodríguez, G. J., Santos-Figueroa, G., Collett, J. L., Decesari, S., Ramos, M. D. C. K. V., Bezerra Netto, H. J. C., De Aquino Neto, F. R. and Mayol-Bracero, O. L.: Speciation of water-soluble inorganic, organic, and total nitrogen in a background marine environment: Cloud water, rainwater, and aerosol particles, J. Geophys. Res. Atmos., 116(5), doi:10.1029/2010JD015010, 2011.

de Gouw, J. A., Middlebrook, A. M., Warneke, C., Goldan, P. D., Kuster, W. C., Roberts, J. M., Fehsenfeld, F. C., Worsnop, D. R., Canagaratna, M. R., Pszenny, A. A. P., Keene, W. C., Marchewka, M., Bertman, S. B. and Bates, T. S.: Budget of organic carbon in a polluted atmosphere: Results from the New England Air Quality Study in 2002, J. Geophys. Res. D Atmos., 110(16), 1–22, doi:10.1029/2004JD005623, 2005.

Grace, D. N., Sharp, J. R., Holappa, R. E., Lugos, E. N., Sebold, M. B., Griffith, D. R., Hendrickson, H. P. and Galloway, M. M.: Heterocyclic Product Formation in Aqueous Brown Carbon Systems, ACS Earth Sp. Chem., 3(11), 2472–2481, doi:10.1021/acsearthspacechem.9b00235, 2019.

Grace, D. N., Lugos, E. N., Ma, S., Griffith, D. R., Hendrickson, H. P., Woo, J. L. and Galloway, M. M.: Brown Carbon Formation Potential of the Biacetyl-Ammonium Sulfate Reaction System, ACS Earth Sp. Chem., 4(7), 1104–1113, doi:10.1021/acsearthspacechem.0c00096, 2020.

Hallquist, M., Wenger, J. C., Baltensperger, U., Rudich, Y., Simpson, D., Claeys, M., Dommen, J., Donahue, N. M., George, C., Goldstein, A. H., Hamilton, J. F., Herrmann, H., Hoffmann, T., Iinuma, Y., Jang, M., Jenkin, M. E., Jimenez, J. L., Kiendler-Scharr, A., Maenhaut, W., McFiggans, G., Mentel, T. F., Monod, A., Prevot, A. S. H., Seinfeld, J. H., Surratt, J. D., Szmigielski, R. and Wildt, J.: The formation, properties and impact of secondary organic aerosol: current and emerging issues, Atmos. Chem. Phys., 9(14), 5155–5236, doi:10.5194/acp-9-5155-2009, 2009.

Hems, R. F. and Abbatt, J. P. D.: Aqueous Phase Photo-oxidation of Brown Carbon Nitrophenols: Reaction Kinetics, Mechanism, and Evolution of Light Absorption, ACS Earth Sp. Chem., 2(3), 225–234, doi:10.1021/acsearthspacechem.7b00123, 2018.

Herrmann, H., Schaefer, T., Tilgner, A., Styler, S. A., Weller, C., Teich, M. and Otto, T.: Tropospheric Aqueous-Phase Chemistry: Kinetics, Mechanisms, and Its Coupling to a Changing Gas Phase, Chem. Rev., 115(10), 4259–4334, doi:10.1021/cr500447k, 2015.

Jerrett, M., Burnett, R. T., Pope, C. A., Ito, K., Thurston, G., Krewski, D., Shi, Y., Calle, E. and Thun, M.: Long-term ozone exposure and mortality, N. Engl. J. Med., 360(11), 1085–1095, doi:10.1056/NEJMoa0803894, 2009.

Juncosa Calahorrano, J. F., Lindaas, J., O'Dell, K., Palm, B. B., Peng, Q., Flocke, F., Pollack, I. B., Garofalo, L. A., Farmer, D. K., Pierce, J. R., Collett, J. L., Weinheimer, A., Campos, T., Hornbrook, R. S., Hall, S. R., Ullmann, K., Pothier, M. A., Apel, E. C., Permar, W., Hu, L., Hills, A. J., Montzka, D., Tyndall, G., Thornton, J. A. and Fischer, E. V.: Daytime Oxidized Reactive Nitrogen Partitioning in Western U.S. Wildfire Smoke Plumes, J. Geophys. Res. Atmos., 126(4), 1–22, doi:10.1029/2020JD033484, 2021.

Khare, P. and Gentner, D. R.: Considering the future of anthropogenic gas-phase organic compound emissions and the increasing influence of non-combustion sources on urban air quality, Atmos. Chem. Phys., 18(8), 5391–5413, doi:10.5194/acp-18-5391-2018, 2018.

Khare, P., Marcotte, A., Sheu, R., Walsh, A. N., Ditto, J. C. and Gentner, D. R.: Advances in offline approaches for trace measurements of complex organic compound mixtures via soft ionization and high-resolution tandem mass spectrometry, J. Chromatogr. A, 1598, 163–174, doi:10.1016/j.chroma.2019.03.037, 2019.

Kieloaho, A. J., Hellén, H., Hakola, H., Manninen, H. E., Nieminen, T., Kulmala, M. and Pihlatie, M.: Gas-phase alkylamines in a boreal Scots pine forest air, Atmos. Environ., 80, 369–377, doi:10.1016/j.atmosenv.2013.08.019, 2013.

Kilian, J. and Kitazawa, M.: The emerging risk of exposure to air pollution on cognitive decline and Alzheimer's disease – Evidence from epidemiological and animal studies, Biomed. J., 41(3), 141–162, doi:10.1016/j.bj.2018.06.001, 2018.

Kim, H., Collier, S., Ge, X., Xu, J., Sun, Y., Jiang, W., Wang, Y., Herckes, P. and Zhang, Q.: Chemical processing of water-soluble species and formation of secondary organic aerosol in fogs, Atmos. Environ., 200(August 2018), 158–166, doi:10.1016/j.atmosenv.2018.11.062, 2019.

Kind, T. and Fiehn, O.: Seven Golden Rules for heuristic filtering of molecular formulas obtained by accurate mass spectrometry., BMC Bioinformatics, 8(1), 105, doi:10.1186/1471-2105-8-105, 2007.

Laskin, A., Laskin, J. and Nizkorodov, S. A.: Chemistry of Atmospheric Brown Carbon, Chem. Rev., 115(10), 4335–4382, doi:10.1021/cr5006167, 2015.

LeClair, J. P., Collett, J. L. and Mazzoleni, L. R.: Fragmentation analysis of water-soluble atmospheric organic matter using ultrahigh-resolution FT-ICR mass spectrometry, Environ. Sci. Technol., 46(8), 4312–4322, doi:10.1021/es203509b, 2012.

Leslie, M. D., Ridoli, M., Murphy, J. G. and Borduas-Dedekind, N.: Isocyanic acid (HNCO) and its fate in the atmosphere: A review, Environ. Sci. Process. Impacts, 21(5), 793–808, doi:10.1039/c9em00003h, 2019.

Li, Y., Pöschl, U. and Shiraiwa, M.: Molecular corridors and parameterizations of volatility in the chemical evolution of organic aerosols, Atmos. Chem. Phys., 16(5), 3327–3344, doi:10.5194/acp-16-3327-2016, 2016.

Liebmann, J., Sobanski, N., Schuladen, J., Karu, E., Hellén, H., Hakola, H., Zha, Q., Ehn, M., Riva, M., Heikkinen, L., Williams, J., Fischer, H., Lelieveld, J. and Crowley, J. N.: Alkyl nitrates in the boreal forest: formation via the NO3-, OH- and O3-induced oxidation of biogenic volatile organic compounds and ambient lifetimes, Atmos. Chem. Phys., 19, 10391–10403, doi:10.5194/acp-2019-463, 2019.

Lim, S., McArdell, C. S. and von Gunten, U.: Reactions of aliphatic amines with ozone: Kinetics and mechanisms, Water Res., 157, 514–528, doi:10.1016/j.watres.2019.03.089, 2019.

Lim, Y. Bin, Kim, H., Kim, J. Y. and Turpin, B. J.: Photochemical organonitrate formation in wet aerosols, Atmos. Chem. Phys., 16(19), 12631–12647, doi:10.5194/acp-16-12631-2016, 2016.

Lin, M., Walker, J., Geron, C. and Khlystov, A.: Organic nitrogen in PM2.5 aerosol at a forest site in the Southeast US, Atmos. Chem. Phys., 10(5), 2145–2157, doi:10.5194/acp-10-2145-2010, 2010.

Lin, P., Laskin, J., Nizkorodov, S. A. and Laskin, A.: Revealing Brown Carbon Chromophores Produced in Reactions of Methylglyoxal with Ammonium Sulfate, Environ. Sci. Technol., 49(24), 14257–14266, doi:10.1021/acs.est.5b03608, 2015.

Di Lorenzo, R. A., Place, B. K., VandenBoer, T. C. and Young, C. J.: Composition of Size-Resolved Aged Boreal Fire Aerosols: Brown Carbon, Biomass Burning Tracers, and Reduced Nitrogen, ACS Earth Sp. Chem., 2(3), 278–285, doi:10.1021/acsearthspacechem.7b00137, 2018.

Loza, C. L., Craven, J. S., Yee, L. D., Coggon, M. M., Schwantes, R. H., Shiraiwa, M., Zhang, X., Schilling, K. A., Ng, N. L., Canagaratna, M. R., Ziemann, P. J., Flagan, R. C. and Seinfeld, J. H.: Secondary organic aerosol yields of 12-carbon alkanes, Atmos. Chem. Phys., 14(3), 1423–1439, doi:10.5194/acp-14-1423-2014, 2014.

Mace, K. A., Kubilay, N. and Duce, R. A.: Organic nitrogen in rain and aerosol in the eastern Mediterranean atmosphere: An association with atmospheric dust, J. Geophys. Res. Atmos., 108(10), doi:10.1029/2002jd002997, 2003a.

Mace, K. A., Artaxo, P. and Duce, R. A.: Water-soluble organic nitrogen in Amazon Basin aerosols during the dry (biomass burning) and wet seasons, J. Geophys. Res. Atmos., 108(16), doi:10.1029/2003jd003557, 2003b.

McNeill, V. F.: Aqueous organic chemistry in the atmosphere: Sources and chemical processing of organic aerosols, Environ. Sci. Technol., 49(3), 1237–1244, doi:10.1021/es5043707, 2015.

Montero-Martínez, G., Rinaldi, M., Gilardoni, S., Giulianelli, L., Paglione, M., Decesari, S., Fuzzi, S. and Facchini, M. C.: On the water-soluble organic nitrogen concentration and mass size distribution during the fog season in the Po Valley, Italy, Sci. Total Environ., 485–486(1), 103–109, doi:10.1016/j.scitotenv.2014.03.060, 2014.

Ng, N. L., Brown, S. S., Archibald, A. T., Atlas, E., Cohen, R. C., Crowley, J. N., Day, D. A., Donahue, N. M., Fry, J. L., Fuchs, H., Griffin, R. J., Guzman, M. I., Herrmann, H., Hodzic, A., Iinuma, Y., Kiendler-Scharr, A., Lee, B. H., Luecken, D. J., Mao, J., McLaren, R., Mutzel, A., Osthoff, H. D., Ouyang, B., Picquet-Varrault, B., Platt, U., Pye, H. O. T., Rudich, Y., Schwantes, R. H., Shiraiwa, M., Stutz, J., Thornton, J. A., Tilgner, A., Williams, B. J. and Zaveri, R. A.: Nitrate radicals and biogenic volatile organic compounds: oxidation, mechanisms, and organic aerosol, Atmos. Chem. Phys., 17(3), 2103–2162, doi:10.5194/acp-17-2103-2017, 2017.

Perring, A. E., Pusede, S. E. and Cohen, R. C.: An Observational Perspective on the Atmospheric Impacts of Alkyl and Multifunctional Nitrates on Ozone and Secondary Organic Aerosol, Chem. Rev., 113(8), 5848–5870, doi:10.1021/cr300520x, 2013.

van Pinxteren, M., Müller, C., Iinuma, Y., Stolle, C. and Herrmann, H.: Chemical Characterization of Dissolved Organic Compounds from Coastal Sea Surface Microlayers (Baltic Sea, Germany), Environ. Sci. Technol., 46(19), 10455–10462, doi:10.1021/es204492b, 2012.

van Pinxteren, M., Fomba, K. W., van Pinxteren, D., Triesch, N., Hoffmann, E. H., Cree, C. H. L., Fitzsimons, M. F., von Tümpling, W. and Herrmann, H.: Aliphatic amines at the Cape Verde Atmospheric Observatory: Abundance, origins and sea-air fluxes, Atmos. Environ., 203, 183–195, doi:10.1016/j.atmosenv.2019.02.011, 2019.

Pope, C. A. and Dockery, D. D.: Health Effects of Fine Particulate Air Pollution: Lines that Connect, J. Air Waste Manage. Assoc., 56, 709–742, doi:10.1080/10473289.2006.10464485, 2006.

Priestley, M., Le Breton, M., Bannan, T. J., Leather, K. E., Bacak, A., Reyes-Villegas, E., De Vocht, F., Shallcross, B. M. A., Brazier, T., Khan, M. A., Allan, J., Shallcross, D. E., Coe, H. and Percival, C. J.: Observations of Isocyanate, Amide, Nitrate, and Nitro Compounds From an Anthropogenic Biomass Burning Event Using a ToF-CIMS, J. Geophys. Res. Atmos., 123, 7687–7704, doi:10.1002/2017JD027316, 2018.

Pye, H. O. T., Nenes, A., Alexander, B., Ault, A. P., Barth, M. C., Clegg, S. L., Collett, J. L., Fahey, K. M., Hennigan, C. J., Herrmann, H., Kanakidou, M., Kelly, J. T., Ku, I. T., Faye McNeill, V., Riemer, N., Schaefer, T., Shi, G., Tilgner, A., Walker, J. T., Wang, T., Weber, R., Xing, J., Zaveri, R. A. and Zuend, A.: The acidity of atmospheric particles and clouds., 2020.

Quinn, P. K., Collins, D. B., Grassian, V. H., Prather, K. A. and Bates, T. S.: Chemistry and Related Properties of Freshly Emitted Sea Spray Aerosol, Chem. Rev., 115(10), 4383–4399, doi:10.1021/cr500713g, 2015.

Rindelaub, J. D., Borca, C. H., Hostetler, M. A., Slade, J. H., Lipton, M. A., Slipchenko, L. V. and Shepson, P. B.: The acid-catalyzed hydrolysis of an α-pinene-derived organic nitrate: Kinetics, products, reaction mechanisms, and atmospheric impact, Atmos. Chem. Phys., 16(23), 15425–15432, doi:10.5194/acp-16-15425-2016, 2016.

Riva, M., Rantala, P., Krechmer, J. E., Peräkylä, O., Zhang, Y., Heikkinen, L., Garmash, O., Yan, C., Kulmala, M., Worsnop, D. and Ehn, M.: Evaluating the performance of five different chemical ionization techniques for detecting gaseous oxygenated organic species, Atmos. Meas. Tech., 12, 2403–2421, doi:https://doi.org/10.5194/amt-12-2403-2019, 2019.

Roberts, J. M., Veres, P. R., VandenBoer, T. C., Warneke, C., Graus, M., Williams, E. J., Lefer, B., Brock, C. A., Bahreini, R., Ozturk, F., Middlebrook, A. M., Wagner, N. L., Dube, W. P. and DeGouw, J. A.: New insights into atmospheric sources and sinksof isocyanic acid, HNCO, from recent urbanand regional observations, J. Geophys. Res. Atmos., 119, 1060–1072, doi:10.1002/2013JD019931, 2014.

Rogers, H. M., Ditto, J. C. and Gentner, D. R.: Evidence for impacts on surface-level air quality in the northeastern US from long-distance transport of smoke from North American fires during the Long Island Sound Tropospheric Ozone Study (LISTOS) 2018, Atmos. Chem. Phys., 20(2), 671–682, doi:10.5194/acp-20-671-2020, 2020.

Ruggeri, G. and Takahama, S.: Technical Note: Development of chemoinformatic tools to enumerate functional groups in molecules for organic aerosol characterization, Atmos. Chem. Phys., 16, 4401–4422, doi:10.5194/acp-16-4401-2016, 2016.

Sander, R.: Compilation of Henry's law constants (version 4.0) for water as solvent, Atmos. Chem. Phys., 15(8), 4399–4981, doi:10.5194/acp-15-4399-2015, 2015.

Sareen, N., Schwier, A. N., Shapiro, E. L., Mitroo, D. and Mcneill, V. F.: Secondary organic material formed by methylglyoxal in aqueous aerosol mimics, Atmos. Chem. Phys., 10, 997–1016, doi:10.5194/acpd-9-15567-2009, 2010.

Schervish, M. and Donahue, N. M.: Peroxy radical chemistry and the volatility basis set, Atmos. Chem. Phys., 20(2), 1183–1199, doi:10.5194/acp-20-1183-2020, 2020.

Schroder, J. C., Campuzano-Jost, P., Day, D. A., Shah, V., Larson, K., Sommers, J. M., Sullivan, A. P., Campos, T., Reeves, J. M., Hills, A., Hornbrook, R. S., Blake, N. J., Scheuer, E., Guo, H., Fibiger, D. L., McDuffie, E. E., Hayes, P. L., Weber, R. J., Dibb, J. E., Apel, E. C., Jaeglé, L., Brown, S. S., Thornton, J. A. and Jimenez, J. L.: Sources and Secondary Production of Organic Aerosols in the Northeastern United States during WINTER, J. Geophys. Res. Atmos., 123(14), 7771–7796, doi:10.1029/2018JD028475, 2018.

Schurman, M. I., Boris, A., Desyaterik, Y. and Collett, J. L.: Aqueous secondary organic aerosol formation in ambient cloud water photo-oxidations, Aerosol Air Qual. Res., 18(1), 15–25, doi:10.4209/aaqr.2017.01.0029, 2018.

Sheu, R., Marcotte, A., Khare, P., Charan, S., Ditto, J. C. and Gentner, D. R.: Advances in offline approaches for chemically speciated measurements of trace gas-phase organic compounds via adsorbent tubes in an integrated sampling-to-analysis system, J. Chromatogr. A, 1575, 80–90, doi:10.1016/j.chroma.2018.09.014, 2018.

Sintermann, J. and Neftel, A.: Ideas and perspectives: On the emission of amines from terrestrial vegetation in the context of new atmospheric particle formation, Biogeosciences, 12(11), 3225–3240, doi:10.5194/bg-12-3225-2015, 2015.

Sodeman, D. A., Toner, S. M. and Prather, K. A.: Determination of Single Particle Mass Spectral Signatures from Light-Duty Vehicle Emissions, Environ. Sci. Technol., 39(12), 4569–4580, doi:10.1016/j.atmosenv.2007.01.025, 2005.

Sullivan, A. P., Guo, H., Schroder, J. C., Campuzano-Jost, P., Jimenez, J. L., Campos, T., Shah, V., Jaeglé, L., Lee, B. H., Lopez-Hilfiker, F. D., Thornton, J. A., Brown, S. S. and Weber, R. J.: Biomass Burning Markers and Residential Burning in the WINTER Aircraft Campaign, J. Geophys. Res. Atmos., 124(3), 1846–1861, doi:10.1029/2017JD028153, 2019.

Takeuchi, M. and Ng, N. L.: Organic nitrates and secondary organic aerosol (SOA) formation from oxidation of biogenic volatile organic compounds, ACS Symp. Ser. Multiph. Environ. Chem. Atmos., 1299, 105–125, doi:10.1021/bk-2018-1299.ch006, 2018.

Tao, Y., Liu, T., Yang, X. and Murphy, J. G.: Kinetics and Products of the Aqueous Phase Oxidation of Triethylamine by OH, ACS Earth Sp. Chem., 5(8), 1889–1895, doi:10.1021/acsearthspacechem.1c00162, 2021.

United States Environmental Protection Agency: Historical Exceedance Days in New England, Reg. 1 EPA New Engl. [online] Available from: https://www3.epa.gov/region1/airquality/standard.html (Accessed 14 August 2021), 2020.

VandenBoer, T. C., Petroff, A., Markovic, M. Z. and Murphy, J. G.: Size distribution of alkyl amines in continental particulate matter and their online detection in the gas and particle phase, Atmos. Chem. Phys., 11(9), 4319–4332, doi:10.5194/acp-11-4319-2011, 2011.

Vidović, K., Lašič Jurković, D., Šala, M., Kroflič, A. and Grgić, I.: Nighttime Aqueous-Phase Formation of Nitrocatechols in the Atmospheric Condensed Phase, Environ. Sci. Technol., 52(17), 9722–9730, doi:10.1021/acs.est.8b01161, 2018.

Warneke, C., McKeen, S. A., de Gouw, J. A., Goldan, P. D., Kuster, W. C., Holloway, J. S., Williams, E. J., Lerner, B. M., Parrish, D. D., Trainer, M., Fehsenfeld, F. C., Kato, S., Atlas, E. L., Baker, A. and Blake, D. R.: Determination of urban volatile organic compound emission ratios and comparison with an emissions database, J. Geophys. Res. Atmos., 112(10), 1–13, doi:10.1029/2006JD007930, 2007.

Wozniak, A. S., Willoughby, A. S., Gurganus, S. C. and Hatcher, P. G.: Distinguishing molecular characteristics of aerosol water soluble organic matter from the 2011 trans-North Atlantic US GEOTRACES cruise, Atmos. Chem. Phys., 14(16), 8419–8434, doi:10.5194/acp-14-8419-2014, 2014.

Wu, C., Wen, Y., Hua, L., Jiang, J., Xie, Y., Cao, Y., Chai, S., Hou, K. and Li, H.: Rapid and highly sensitive measurement of trimethylamine in seawater using dynamic purge-release and dopant-assisted atmospheric pressure photoionization mass spectrometry, Anal. Chim. Acta, 1137, 56–63, doi:10.1016/j.aca.2020.08.060, 2020.

Xu, Y., Miyazaki, Y., Tachibana, E., Sato, K., Ramasamy, S., Mochizuki, T., Sadanaga, Y., Nakashima, Y., Sakamoto, Y., Matsuda, K. and Kajii, Y.: Aerosol Liquid Water Promotes the Formation of Water-Soluble Organic Nitrogen in Submicrometer Aerosols in a Suburban Forest, Environ. Sci. Technol., 54(3), 1406–1414, doi:10.1021/acs.est.9b05849, 2020.

Ye, C., Zhou, X., Pu, D., Stutz, J., Festa, J., Spolaor, M., Tsai, C., Cantrell, C., Mauldin, R. L., Campos, T., Weinheimer, A., Hornbrook, R. S., Apel, E. C., Guenther, A., Kaser, L., Yuan, B., Karl, T., Haggerty, J., Hall, S., Ullmann, K., Smith, J. N., Ortega, J. and Knote, C.: Rapid cycling of reactive nitrogen in the marine boundary layer, Nature, 532, 489–491, doi:10.1038/nature17195, 2016.

Youn, J. S., Crosbie, E., Maudlin, L. C., Wang, Z. and Sorooshian, A.: Dimethylamine as a major alkyl amine species in particles and cloud water: Observations in semi-arid and coastal regions, Atmos. Environ., 122, 250–258, doi:10.1016/j.atmosenv.2015.09.061, 2015.

Yu, L., Smith, J., Laskin, A., M George, K., Anastasio, C., Laskin, J., M Dillner, A. and Zhang, Q.: Molecular transformations of phenolic SOA during photochemical aging in the aqueous phase: Competition among oligomerization, functionalization, and fragmentation, Atmos. Chem. Phys., 16(7), 4511–4527, doi:10.5194/acp-16-4511-2016, 2016.

Zhang, J., Ninneman, M., Joseph, E., Schwab, M. J., Shrestha, B. and Schwab, J. J.: Mobile Laboratory Measurements of High Surface Ozone Levels and Spatial Heterogeneity During LISTOS 2018: Evidence for Sea Breeze Influence, J. Geophys. Res. Atmos., 125(11), 1–12, doi:10.1029/2019JD031961, 2020.

Zhang, Q., Anastasio, C. and Jimenez-Cruz, M.: Water-soluble organic nitrogen in atmospheric fine particles (PM2.5) from northern California, J. Geophys. Res. D Atmos., 107(11), 1–9, doi:10.1029/2001jd000870, 2002.

Zhao, Y., Hallar, A. G. and Mazzoleni, L. R.: Atmospheric organic matter in clouds: Exact masses and molecular formula identification using ultrahigh-resolution FT-ICR mass spectrometry, Atmos. Chem. Phys., 13(24), 12343–12362, doi:10.5194/acp-13-12343-2013, 2013.

Zhou, S., Collier, S., Xu, J., Mei, F., Wang, J., Lee, Y.-N., Sedlacek, A. J., Springston, S. R., Sun, Y. and Zhang, Q.: Influences of upwind emission sources and atmospheric processing on aerosol chemistry and properties at a rural location in the Northeastern U.S., J. Geophys. Res. Atmos., 121(10), 6049–6065, doi:10.1002/2015JD024568, 2016.